This is to certify that the
thesis entitled

ELECTROSPRAY IONIZATION MASS SPECTROMETRY FOR THE DETECTION AND CHARACTERIZATION OF SMOKELESS POWDER

presented by

Gwynyth Scherperel

has been accepted towards fulfillment
of the requirements for the

M.S. degree in Criminal Justice

Ruth Waddell
Major Professor's Signature

31 AUGUST 2007
Date

ELECTROSPRAY IONIZATION TANDEM MASS SPECTROMETRY FOR THE DETECTION AND CHARACTERIZATION OF SMOKELESS POWDERS

BY

GWYNYTH SCHERPEREL

A THESIS

Submitted to
Michigan State University
In partial fulfillment of the requirements
For the degree of

MASTER OF SCIENCE

Department of Criminal Justice

2007

ABSTRACT

ELECTROSPRAY IONIZATION TANDEM MASS SPECTROMETRY FOR THE DETECTION AND CHARACTERIZATION OF SMOKELESS POWDERS

BY

GWYNYTH SCHERPEREL

Smokeless powder is one of the most common types of explosives used today in civilian ammunition and because of this it is also commonly found in improvised explosive devices. Thus, the detection of smokeless powder in the form of unexploded powder or residue from a gunshot or post-blast explosion can be of great forensic value. Tandem mass spectrometry (MS/MS and MS^n) in a quadrupole ion trap with electrospray ionization was examined in order to develop a method for the routine, rapid identification and comparison of smokeless powder. This method was optimized for the simultaneous detection of the smokeless powder stabilizers methyl centralite, ethyl centralite, and diphenylamine and it was found that good limits of detection could be achieved for all three stabilizers. Seven smokeless powder samples and their residues were then analyzed as 'real world' samples. The use of tandem mass spectrometry and selected reaction monitoring increased the sensitivity and selectivity, respectively, of this technique for both the unburned and burned powders, allowing for the identification of trace components. Mass spectrometry was able to identify all of the unburned powder samples as being smokeless and it was able to identify gunshot residue at firing distances of 3" and 12" on unwashed, hand washed (in deionized water), and machine washed cloth. All but two of the unburned powders could be differentiated from each other by combining the mass spectrometry data with the physical characteristics and extraction tendencies of the smokeless powders.

ACKNOWLEDGMENTS

This project would not have been possible without the support of many people. First, I would like to thank my research advisor, Dr. Ruth Waddell, for her guidance, encouragement, and support. I would also like to thank my committee members, Dr. Gavin Reid and Dr. Vince Hoffman. A special thanks goes to Dr. Reid for allowing me to use his lab equipment, chemicals, and space, without which this project would not have been possible, and for all of his guidance and support throughout my graduate studies. This project could also not have been completed without the help of the certified firearm instructor employed by the Michigan State University Police Department who provided all of the ammunition and firearms used and who allowed us access to the Michigan State Police firing range where he was gracious enough to fire the bullets, providing us with an unending supply of gunshot residue. I would also like to thank previous and current group members of the Reid research group and the forensic chemistry graduate students for their friendship, help, and motivation. Finally, I would like to thank my parents and friends who endured this long process with me, always offering support and encouragement.

TABLE OF CONTENTS

LIST OF FIGURES

LIST OF TABLES

LIST OF SCHEMES

CHAPTER ONE

Introduction

1.1 Smokeless Powder

One of the most common types of propellant used in civilian ammunition today is smokeless powder. Smokeless powder, as are all gunpowders, is a low explosive, meaning that it deflagrates rather than detonates [1, 2]. Deflagration is a subsonic combustion (less than 1100 ft/s) that spreads by thermal conductivity, *i.e.*, burning material heats and subsequently ignites surrounding cold material. Detonation, on the other hand, is a supersonic combustion (greater than 1100 ft/s) that creates shock waves that compress cold material causing its temperature to rise to the ignition point (shock compression) [3, 4]. Since smokeless powder is used for civilian ammunition and can be legally purchased for reloading, this propellant is one of the most common low explosives used to make improvised explosive devices (IEDs), such as pipe bombs [3-6]. The majority of homicides, aggravated assaults, and robberies in the United States today are committed using handguns, which consist of pistols and revolvers [7]. Thus, the detection of smokeless powder in the form of unexploded powder or in residue form from a gunshot or post-blast explosion can have significant forensic value.

1.2 Current Applications of Smokeless Powder

1.2.1 Ammunition

A firearm cartridge, as illustrated in Figure 1.1 below, consists of a projectile (the bullet), a primer (explosive cap), a propellant (gunpowder), and a casing that holds everything together [8].

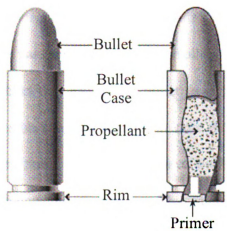

Figure 1.1 Components of a modern cartridge. (Adapted from "How Revolvers Work". www.howstuffworks.com).

Bullet designs and compositions vary by function. For maximum efficiency, *i.e.*, to cause the greatest damage, a bullet should sufficiently penetrate a target to immobilize it without completely passing through it. Most bullets consist of a relatively soft lead or lead alloy core and can be jacketed, semi-jacketed, or non-jacketed [8, 9]. A jacketed bullet has a hard metal coating, such as copper, over the lead core. This gives the bullet strength allowing it to deeply penetrate targets more, making it an ideal bullet for such applications as armor piercing. On the other hand, a non-jacketed bullet consists of only the soft lead core making the bullet structurally weaker than the jacketed bullets and

therefore less likely to pass through a target such as small game [8, 9]. The caliber of a bullet refers its diameter in either mm or inches.

The shape of a bullet dictates its aerodynamic and impact characteristics. The three primary shapes are solid-nosed, hollow point, and soft-nosed (or soft point) [8]. The end of a solid-nosed bullet is round and blunted and is therefore likely to stay in its original shape even after striking a target. As was the case for jacketed bullets, this is ideal for such purposes as armor piercing, but not for small game hunting where this type of bullet is apt to completely pass through a target. Hollow point bullets have a hollow cavity in the nose of the bullet that causes the bullet to expand ('mushroom') when a target is struck. This expansion causes the bullet to slow down inside the target. Soft-nosed bullets fall in between these two as this type of bullet expands slower than the hollow point bullets do upon impact with a target. This causes the bullet to penetrate the target further than hollow point bullets, but less than the solid-nosed bullets [8].

The primer consists of a stable but shock-sensitive mixture that ignites when struck. The primary components are typically lead (Pb) styphnate (initiating explosive), barium (Ba) nitrate (oxidizing agent), and antimony (Sb) sulfide (fuel) [8]. When the trigger of a firearm is pulled, a series of actions takes place within the firearm that results in a firing pin hitting the back of the cartridge, igniting the primer. This in turn deflagrates the gunpowder, which expands and pushes the bullet out the path of least resistance (*i.e.*, the barrel of the firearm). Smokeless powder has widely replaced black powder as the primary propellant (*i.e.*, gunpowder) used in civilian ammunition due to its higher efficiency and smokeless nature, meaning that the primary combustion products are gaseous, leaving minimal residue in the barrel of the gun [3]. Thus, from a forensic

perspective, one is more likely to encounter smokeless powder than black powder when dealing with firearm related cases.

1.2.2 Improvised Explosive Devices (IEDs)

A pipe bomb is simply a pipe that contains an explosive material. It is a common form of improvised explosive device (IED) because of the relative ease in which the supplies can be obtained and assembled. Pipe bombs have become more prominent in the public eye lately as they have been used in many high profile cases, such as the terrorist attacks on U.S. soldiers in Iraq [10]. The United States Bureau of Alcohol, Tobacco, Firearms, and Explosives reported more than half of their explosive cases involved pipe bombs and about 50% of those used smokeless powder as the explosive [6]. Even though smokeless powder is a low explosive, when it is contained in a closed container, the large volume of gases created upon ignition will cause the container to burst in a relatively large explosion and release fragmented debris (shrapnel). Thus, while simple, pipe bombs can cause considerable damage, as exemplified in the Centennial Olympic Park bombing, which involved pipe bombs made with smokeless powder. Sharp objects, such as nails or screws, can also be incorporated into a pipe bomb in order to increase the amount of shrapnel, making the pipe bomb even more dangerous.

1.3 Manufacturing and Components of Smokeless Powder

Smokeless powder can be widely classified as single-based, double-based, or triple-based according to the major component(s) of the powder. Single-based powder

consists of nitrocellulose, while double-based powder contains nitrocellulose and nitroglycerine, which is added as a plasticizer in order to soften the propellant and raise the energy content. Triple-based powder contains nitroguanadine in addition to nitrocellulose and nitroglycerine. Triple-based smokeless powders, however, are used primarily in rockets and large caliber military grade weapons and are therefore difficult to obtain on the open market [1, 11].

Smokeless powders also contain many minor ingredients, such as flash suppressants, deterrents, opacifiers, plasticizers, and stabilizers [2]. Flash suppressants, which are commonly alkali or alkaline earth salts, help prevent secondary flash at the muzzle of the firearm [8]. Deterrents coat the exterior of the propellant granules to increase efficiency. Deterrents include such compounds as dioctyl phthalate and dinitrotoluene. Opacifiers, the most common of which is carbon black, enhance reproducibility of the burn rate. Plasticizers soften the propellant and reduce hygroscopicity. Examples of plasticizers include nitroglycerine, dibutyl phthalate, and dinitrotoluene [12, 13]. Stabilizers are added to slow down the decomposition of nitrocellulose by removing the nitrous and nitric acids that are produced. These decomposition products catalyze further decomposition of nitrocellulose, but if they are removed the decomposition is relatively slow [14]. Common stabilizers used today are diphenylamine (DPA), methyl centralite (MC), and ethyl centralite (EC) [12].

It is not possible to predict the composition of a powder based on the caliber or bullet type. This is because sub-batches of commercial powders are blended during the manufacturing of the powder in order to achieve the desired propellant performance and stability [3, 11, 15]. Each batch of powder may also consist of 'rework'; powder that did

not meet specifications or was recycled [16, 17]. This blending of batches combined with the addition of 'rework' can lead to compositional heterogeneity (qualitative and quantitative) between commercially available cartridges [6, 18, 19]. This, however, allows for the development of distinct chemical profiles for different powders [5, 6, 20].

1.4 Current Methods for the Forensic Detection and Analysis of Smokeless Powder

Unburned smokeless powders are initially characterized by their morphology, but powders are also distinguishable based on the presence or absence of certain compounds [21]. Thus, the physical and chemical characteristics of smokeless powder can help associate or differentiate unknown powders with residue (gunshot or post-blast) or with known powder samples [6, 11, 18, 19, 22, 23]. The agreement in composition between burned and unburned powder is generally very good [11, 18, 22], but the level of association will depend on the rarity of the composition of the powder [13]. Chemical characteristics can also be used to identify gunshot residue or to identify the type of powder used in an explosive. There have been a number of methods for the analysis of smokeless powders that have been examined. These procedures have been extensively reviewed [1, 3] and only a brief discussion follows.

1.4.1 Gunshot Residue (GSR)

Gunshot residue (GSR) is primarily a mixture of burned, partially burned, and unburned primer and propellant particles, but it can also include particles from the bullet, casing, and firearm [12, 24]. The exact composition will depend on a number of factors,

including the firearm and ammunition used (type, caliber, age, *etc.*). GSR can be deposited on any object or person that is near the gun when it is fired [8, 12]. The persistence of propellant residue on clothing, however, is considerably longer than it is on skin or hair, resulting in a higher probability of its detection and identification when it is on cloth [8, 13, 25]. The detection of GSR can help determine if a suspect has recently fired a gun, help discriminate between homicide and suicide by the location of GSR on the victim and/or suspect, induce a confession or admission, and assist in determining cause of death [12]. GSR can also help identify a shooter by comparing the composition of the GSR with that of unfired propellant found in the suspect's possession. This is especially useful if the weapon, bullet, or both are not found or are too badly damaged for analysis [12].

The two primary approaches used today for the analysis of gunshot residue are color tests (*i.e.*, modified Griess test and sodium rhodizonate test) and scanning electron microscopy coupled with energy dispersive x-ray analysis (SEM/EDX) [24].

1.4.1.1 Color Tests

These chromophoric techniques aid in the visualization of gunshot residue by producing a visible color reaction with components in GSR [8, 24]. The modified Griess test (MGT) is a test for the detection of nitrite compounds [26]. Nitrite compounds are formed when smokeless powder is burned and thus can appear in gunshot residue. This test will yield a positive result if any nitrite is present. Thus, the possibility for a false positive is significant since nitrites exist is some everyday items such as deodorizers and disinfectants [13]. The sodium rhodizonate test (SRT) is used to determine the presence

of lead, which can be present in GSR from the primer, from a lead bullet/barrel interaction, or from surface erosion of the bullet's base [13]. As was the case for the MGT, the SRT will give a positive result for the presence of any lead compounds, not just those from GSR. Thus, these color tests lack the specificity desired for definitive forensic identification of GSR [15].

1.4.1.2 Scanning Electron Microscopy/Energy Dispersive X-ray Analysis (SEM/EDX)

SEM/EDX can be used to simultaneously determine a particle's morphology (SEM) and elemental composition (EDX). GSR particles produced from the primer have a distinct spherical shape making them detectable under the high magnification of SEM. They also contain characteristic components of the primer, Pb, Ba, and Sb, that can be detected by EDX [8, 12]. It is this combination of Pb, Ba, and Sb in a single particle that is considered characteristic of GSR, while other combinations are considered to be consistent with, but not unique to, GSR [12, 24]. SEM/EDX, however, can be very time consuming (8-12 hours) as the analyst must search and locate GSR particles over a large surface area potentially covered in non-firearm related debris (such as dirt and skin) [8, 12]. This has in some part, however, been overcome by automated instrumentation [12, 13], but even the automated system can take 2-3 hours to search debris on one item [8, 27].

Another pitfall with SEM/EDX is due to the recent development of heavy metal-free primers that were introduced due to the growing environmental and health concerns over leaded ammunition [22]. More common metals such as zinc and strontium are now

used in primers, but these metals alone are not specific to GSR. Therefore, other means of identifying GSR must be explored [12, 22].

1.4.2 Improvised Explosive Device (IED) Post-blast Residue

The recent increase in terrorist activity [10] has elevated the need for analytical methods that can accurately identify explosives and post-blast explosive residue, as this may provide a crucial link between an explosive and a suspect. Post-blast residue may be found on a suspect's clothing, skin, or hair and can be compared with the powder and/or residue found at the scene of an explosion. Another forensically important determination in any bombing is the type of explosive used, which can be determined by analyses of the powder's chemical composition; the use of taggants was recently deemed impractical and unnecessary, as it is possible to use chemical composition for identification [3, 16, 19]. Thus, post-blast residues can be, and typically are, collected and analyzed for their additive content as a means of characterizing and identifying powders [5, 6, 17]. Two main laboratory methods utilized for detection of post-blast residue are gas chromatography/mass spectrometry (GC/MS) and gas chromatography with a thermal energy analyzer (GC/TEA) [13], but these techniques have limitations as discussed in the following section.

1.5 Developing Methods for the Detection and Analysis of Smokeless Powder by Identifying Organic Components

While definitive results for GSR can be obtained by SEM/EDX, analysis of organic residues can provide complementary or additional information, especially if

inorganic components are not found or are inconclusive [12, 19]. Thus one new promising approach is the analysis of the organic additives in smokeless powder because this can not only be used for the detection of firearm use, but it can also be used to identify the powder used in an IED and it can be used to provide composition information that can potentially associate residues and unfired powder. The three most commonly used stabilizers in smokeless powder, MC, EC, and DPA, are regarded as being the most characteristic organic material in smokeless powder [15, 28, 29].

EC and MC are found in celluloid and solid rocket propellant [12, 16], while DPA is used in rubber products and in the food industry [14, 29]. Since there are environmental contamination possibilities for all these compounds the simultaneous identification of a number of additives may be required for unambiguous forensic identification and association [16]. The presence of nitrated derivatives of DPA, however, is considered virtually unique to GSR because industrial and environmental uses of DPA are not normally associated with nitrating agents [14, 29]. DPA is nitrated by the nitrogen oxides released by the degradation of nitrocellulose to form various nitro- and nitroso- derivatives, including 2-nitroDPA, 4-nitroDPA, and N-nitrosoDPA [11, 14, 29].

The thermal instability of most explosives and the need for high sensitivity due to the low concentration of stabilizer in smokeless powder, limits the number of analytical methods that can be used [27, 28, 30, 31]. Gas chromatography (GC) and liquid chromatography (LC) are the most commonly used techniques, coupled with a variety of detectors including ultraviolet (UV), thermal energy analyzer (TEA), electron capture detector (ECD), and mass spectrometry (MS) [30]. UV detectors are nonselective and are only good at trace levels for detection of materials that absorb strongly in the UV range.

TEA is also nonselective. ECD has good limits of detection for nitro compounds, but its linearity and sensitivity are significantly dependent on the electron capture properties of the solvent and any impurities. A detection system that can overcome the disadvantages of UV, TEA, and ECD is mass spectrometry, which is both sensitive and selective [30]. GC/MS and LC/MS have been reported by many groups and labs for the analysis of smokeless powder [12, 16, 17, 30, 32, 33]. Wu *et al.* used HPLC with a triple quadrupole mass spectrometer in order to analyze standard solutions of MC and nitroglycerine (NG) as well as GSR extracted from gloves worn by a shooter [31]. By using tandem mass spectrometry and multiple reaction monitoring (MRM), few interfering peaks were seen.

Chromatography techniques, however, are not without problems for explosive analysis. GC is disadvantageous due to the instability and thermal degradation of some nitrated components, such as DPA and its derivatives [5, 20, 33]. While the thermally unstable and non-volatile constituents of smokeless powders can by analyzed by LC [11], isocratic LC methods are limited due to the wide range of components' polarities and difficulty in separating geometric isomers [5, 20]. These disadvantages have led to the development of some alternative methods. A gradient reversed-phase liquid chromatography – electrospray ionization mass spectrometry (LC-ESI-MS) method using a quadrupole ion trap mass spectrometry has been developed. [21]. There have also been studies that do not utilize any chromatography system. A triple quadrupole mass spectrometer with electrospray ionization and a flow-injection system (C18 column) was used to examine MC standards and GSR extracted directly from shooters' skin [28]. In another study by this same group, a triple quadrupole mass analyzer with ESI interface was successfully used to examine standard solutions of DPA and its nitrated derivates

along with GSR extractions from skin [29]. These previous ESI-MS studies, however, were limited in the number of additives detected at any given time.

1.6 Aims of this Thesis

The aims of this thesis are:

1. to develop and optimize a method for the identification of the organic stabilizers commonly found in smokeless powders (MC, EC, DPA, and DPA nitrated derivates) by nanoelectrospray ionization tandem mass spectrometry (nESI-MS/MS) with a quadrupole ion trap,
2. to develop a rapid and efficient technique for the extraction of organic stabilizers from small samples of smokeless powder,
3. to characterize and differentiate unburned smokeless powders based on their physical appearances, extraction yields, and mass spectra, and;
4. to use nESI-MS/MS to analyze gunshot residue obtained at different firing distances for the existence of the stabilizers MC, EC, and DPA and to compare this with the known source powder.

CHAPTER TWO

Mass Spectrometry

2.1 Mass Spectrometry

Mass spectrometry involves the ionization, separation, and detection of a sample in order to determine the characteristic ions present by measuring their mass-to-charge ratios (m/z). The speed, sensitivity, and specificity of mass spectrometry make it particularly attractive for use in forensic applications. A mass spectrometer consists of the components illustrated in Figure 2.1.

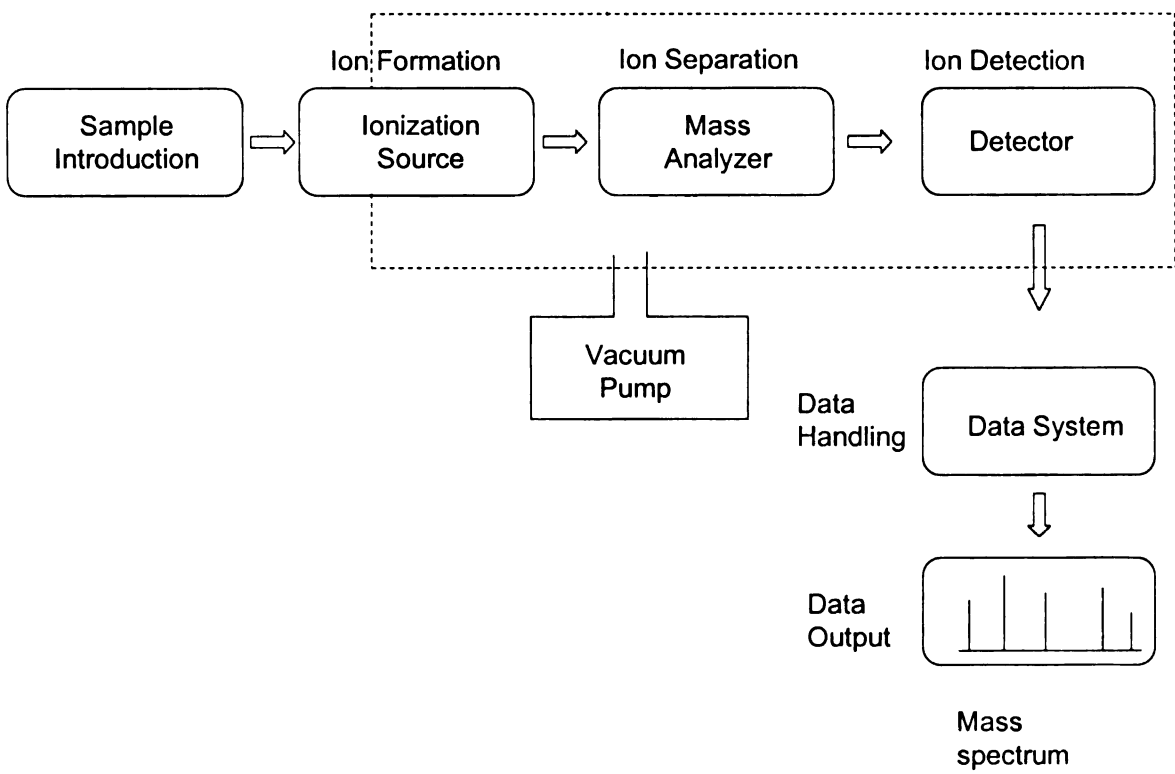

Figure 2.1 Components of a mass spectrometer (adapted from "What is Mass Spectrometry". www.asms.org).

2.1.1 Ionization

2.1.1.1 Electrospray Ionization (ESI)

The first component of a mass spectrometer is the ionization source, which is responsible for the conversion of molecules to ions. During the mid 1980's, electrospray ionization (ESI), a 'soft' ionization technique, was developed by Fenn *et al.* [34]. ESI, illustrated in Figure 2.2, involves dissolving the sample in a liquid solvent and then pumping this through a small diameter capillary tubing. The capillary tip, located at atmospheric pressure, is floated at high potential causing the formation of an electric field which induces charge accumulation at the surface of the liquid. When a high enough voltage is applied to break the surface tension of the solvent, a Taylor cone forms and an electrospray of charged droplets begins. Gaseous ions are then produced as these charged droplets undergo solvent evaporation, due to high temperature or the presence of a sheath gas, and coulomb fissions, due to either the charge residue model (CRM) [35] or the ion evaporation model (IEM) [36, 37].

The CRM argues that a sequence of Rayleigh instabilities (where columbic repulsion becomes greater than the surface tension) and periods of solvent evaporation produce final droplets that contain only one ion each. This ion is then liberated into a gas-phase ion as the last of the solvent evaporates. The IEM, on the other hand, proposes that before a droplet reaches the final stage in the CRM model, where it contains only one ion, the field on the droplet's surface becomes strong enough to overcome the solvation forces, allowing an ion to escape from the droplet surface and enter the gas phase. It is thought that large molecules ionize according to the CRM, while the dominant mechanism for smaller molecules may be the IEM [38].

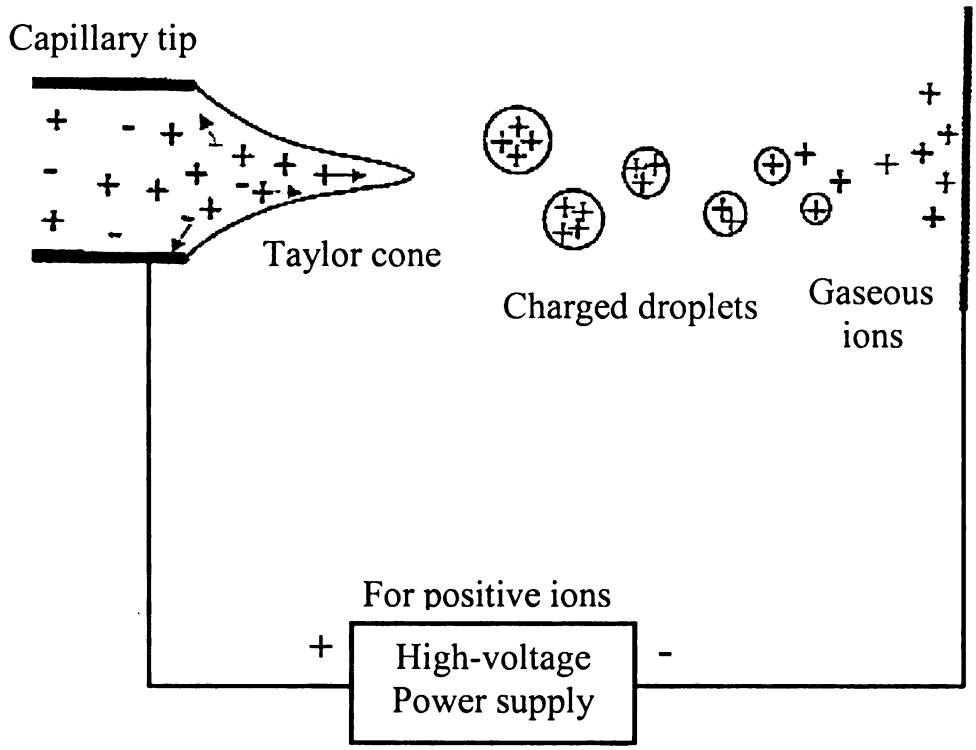

Figure 2.2 Schematic of electrospray ionization (ESI). (Reproduced and modified from reference 42)

ESI can be coupled with high performance liquid chromatography (HPLC) or used in a direct infusion mode. When coupled with HPLC, the analytes are dissolved in the appropriate HPLC solvent and are subjected to ESI directly as they elute from the column. While HPLC is not always applicable in forensic work, its advantages are that it is a separation technique that offers another possible means of identifying an unknown (retention time) and it is amendable to high throughput because it can be automated. In the direct infusion mode, analytes are dissolved in an appropriate solvent, such as methanol/water (1:1), and introduced into the mass spectrometer at the desired flow rate via a syringe pump. Nanoelectrospray ionization (nESI) uses less solution than

conventional ESI by running at a lower flow rate, ~1 μL/min or less, and takes advantage of the smaller droplet sizes [39].

2.1.1.2 Matrix-assisted Laser Desorption Ionization (MALDI)

Matrix-assisted laser desorption ionization (MALDI) was developed in the late 1980's by Karas and Hillenkamp [40]. MALDI utilizes the impact of high energy photons from a laser on a sample imbedded in a solid organic crystalline matrix to ionize analytes. First, the sample is dissolved in a matrix containing a UV absorbing chromophore and crystallized onto a metal target. This target is then placed under vacuum in the ion source and bombarded with short duration laser pulses. This causes the sample to heat up and the sample and matrix to sublime. While the exact mechanism of ionization has been the subject of much discussion [41], it is generally accepted that it is the interaction of the laser pulse with the samples that results in the ionization of both matrix and the analyte molecules. In contrast to ESI, MALDI predominantly produces pseudomolecular ions that are singly charged. Although ESI was exclusively employed in the studies reported herein, MALDI is a sensitive ionization technique, and would likely serve as a complementary ionization technique for the analysis of smokeless powders.

2.1.2 Mass Analyzers

The purpose of the mass analyzer component of the mass spectrometer is to separate mixtures of gas-phase ions according to their m/z ratios. A range of mass analyzers exists for this purpose, each with their own unique capabilities and operational

performance characteristics (*e.g.*, resolution, sensitivity, mass accuracy). Three types of mass analyzers commonly used in forensic analyses are: (i) quadrupole, (ii) triple quadrupole, and (iii) quadrupole ion trap. The quadrupole ion trap analyzer, which was used in this study, is discussed in the following section.

2.1.2.1 The Quadrupole Ion Trap Mass Analyzer

The quadrupole ion trap is an electrodynamic mass analyzer consisting of a ring electrode and two end caps, as illustrated in Figure 2.3. A variable amplitude radio frequency (RF) is applied to the ring electrode to create a three dimensional quadrupole electric field to trap ions within the region bound by the electrodes. By adding a small amount of bath gas, such as helium, the motion of ions injected into the trap can be dampened, thereby increasing their trapping efficiency.

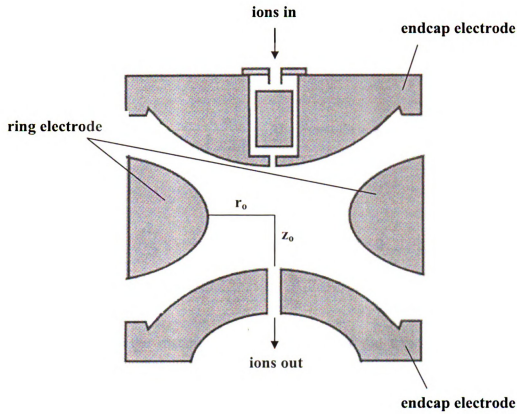

Figure 2.3 Diagram of a quadrupole ion trap. (Reproduced and modified from reference 43)

The potential applied to the ring electrode can be given by the equation

$$\Phi_0 = + (U\text{-}V\cos \omega t) \quad (1)$$

where U is the amplitude of the direct current (DC) potential, V is the amplitude of the applied alternating current (AC) potential (in the RF range), ω is the angular frequency ($\omega = 2\pi\upsilon$, where υ is the frequency of the applied RF), and t is time. The field is seen in three dimensions, thus the motion of the ions under the influence of the applied potentials occurs in three dimensions: x, y, and z. Due to the cylindrical symmetry of the trap x

equals y and the ion motion can be expressed using the coordinates z and r. Thus, the equations of motion inside the trap can be shown to be

$$\frac{d^2z}{dt^2} - \frac{4e}{m\left(r_0^2 + 2z_0^2\right)}(U - V\cos\omega t)z = 0 \tag{2}$$

$$\frac{d^2r}{dt^2} + \frac{2e}{m\left(r_0^2 + 2z_0^2\right)}(U - V\cos\omega t)r = 0 \tag{3}$$

where r_o and z_o are the distances from the center of the trap to the ring and exit electrodes, respectively, and **z** is the charge on the ion.

Similarities can be seen when comparing these two equations with the Mathieu equation, which describes the propagation of waves in membranes, given below.

$$\frac{d^2u}{d\xi^2} + (a_u - 2q_u\cos 2\xi)u = 0 \tag{4}$$

In equation (4), u can stand for either z or r in equations (2) and (3) and $\xi = \frac{\omega t}{2}$. Thus, the equations of ion motion in the ion trap given can be written in the form of the Mathieu equation:

$$a_U = a_Z = -2a_r = \frac{-16zeU}{m(r_0^2 + 2z_0^2)\omega^2} \tag{5}$$

$$q_u = q_z = -2q_r = \frac{4zeV}{mr_0^2\omega^2} \tag{6}$$

$$q_z = \frac{8zeV}{m(r_0^2 + 2z_0^2)\omega^2} \tag{7}$$

where U is the DC potential, V is the amplitude of the RF potential, m is the mass of an ion, r_o is the distance from the center of the trap to the ring electrode, z_o is the distance from the center of the trap to the exit electrodes, and ω is the angular velocity of the RF potential; r_o, z_o, and ω are constant for a given trap.

There is no applied DC potential in three dimensional ion trap mass analyzers, thus the a_u term from the Mathieu equation equals zero. The solution for the dimensionless trapping parameter q_u (related to the RF potential, V) is therefore the critical parameter. Equation (6) is the solution for an ideal ion trap, while equation (7) is for a 'stretched' quadrupole ion trap [43]. A 'stretched' trap is one where the distance between the end caps has been increased to introduce a negative higher order field (*i.e.*, octapole) component to offset the positive higher order field introduced by truncation of the potential field from the ion trap electrodes.

Ions are stable in the ion trap as long as their trajectories do not reach the distances r_0 and z_0 (Figure 2.3). By plotting a_u versus q_u, the areas where ions of a given mass-to-charge ratio (m/z) are stable, *i.e.*, do not reach values above or equal to r_0 or z_0, as a function of the applied RF frequency and amplitude, can be determined. Figure 2.4 shows such a stability diagram for a 3D quadrupole ion trap [42]. As there is no applied DC potential, all of the ions line up along the x-axis of the stability diagram. According

to equations (6) and (7), q is directly proportional to V, but inversely proportional to m/z. Thus, for a given m/z, as V is increased ions move along the x-axis towards higher q values. Ions will become unstable as they reach the boundary of the stability region, at a q value of 0.908, and will be ejected from the trap. Thus, a mass spectrum may be acquired by scanning the amplitude of the RF field (V) applied to the ring electrode to progressively destabilize ions of increasing m/z value. This, however, is not the most efficient manner to eject ions from a trap because several m/z ions can be ejected at essentially the same time due to the slope of the potential well in which ions are trapped (discussed later), thereby resulting in loss of resolution.

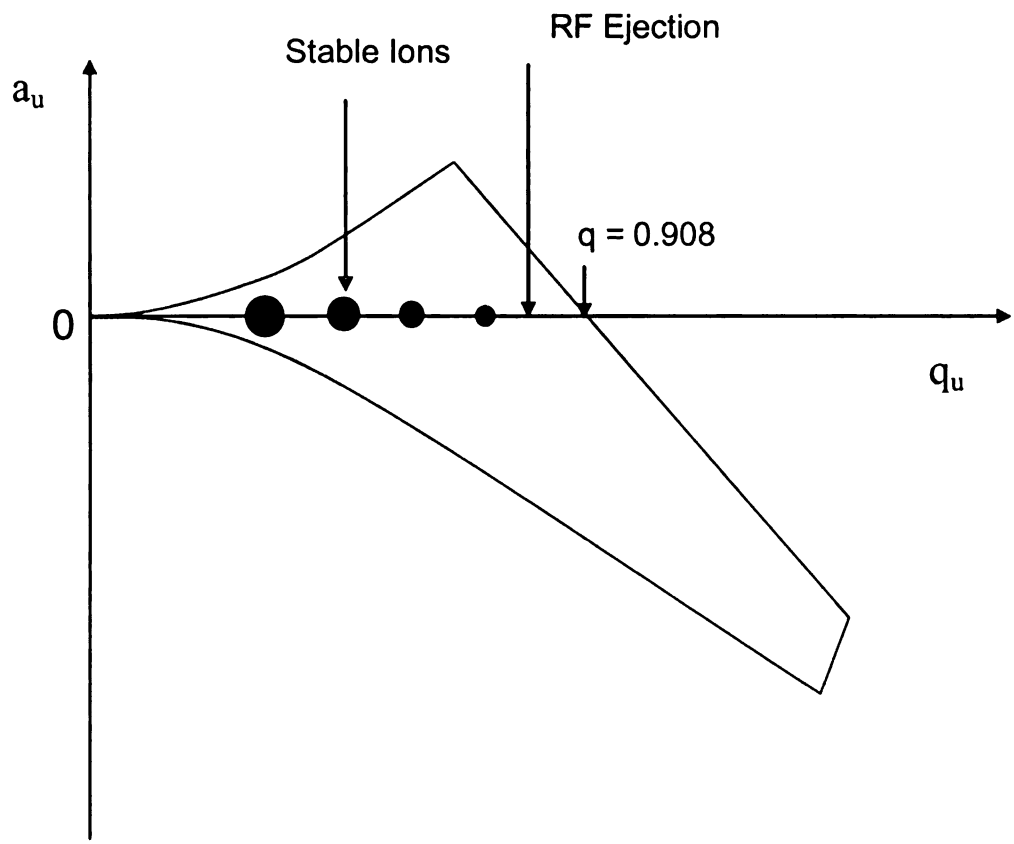

Figure 2.4 Typical Mathieu stability diagram for quadrupole ion trap. The larger balls represent high mass ions whereas the smaller balls represent low mass ions. (Reproduced and modified from reference 42)

One solution to overcome this is to use resonance ejection. It was noted earlier that υ is the frequency of the applied RF field. Ions in the trap, however, do not oscillate at this fundamental frequency because of their inertia. They will oscillate at a secular frequency f that is lower than υ. The relationship between f and υ along the z axis is given by

$$f_z = \frac{\beta_z v}{2} \tag{8}$$

where β_z is a fundamental stability parameter given by the approximation

$$\beta_u = \left[a_u + \left(\frac{q_u^2}{2} \right) \right]^{1/2} \tag{9}$$

for q_u values lower than 0.4. Since β_z equals one at the q value of 0.908 (where ions become unstable), the maximum secular frequency an ion can have is half the applied RF frequency. If a supplementary auxiliary AC (RF) signal, or 'tickle', is applied to the endcap electrodes, typically at a q value of 0.86, an ion's secular frequency can be slowly raised (by increasing V) until it matches the applied frequency on the endcaps, *i.e.*, it is in resonance with the AC signal, and is ejected.

The multistage tandem mass spectrometry (MS/MS and MS^n) capabilities of the ion trap make it particularly attractive as a mass analyzer for trace analysis studies by improving both the signal-to-noise ratio (S/N) and detection limits. Tandem mass

spectrometry involves the repeated isolation and fragmentation of ions, which occurs n times for an MS^n analysis. For example, an MS/MS experiment would involve a series of events consisting of isolation of a precursor ion, an intermediate reaction event (typically involving energetic dissociation), followed by mass analysis of the product ions [44]. Isolation of the selected precursor ion is performed by the application of a high amplitude 'notched' broadband resonance ejection supplementary RF signal applied to the end caps in order to eject all ions except the precursor ion of interest. The isolated ion is then subjected to fragmentation by collision induced dissociation (CID), through the application of a low amplitude RF resonance excitation signal applied to the end cap electrodes. This signal is at a frequency corresponding to the secular frequency of motion of the ion of interest, enabling energetic collisions with the background He gas that is present. This causes a fraction of the kinetic energy to be converted into internal energy, bringing the ion to a vibrationally excited state and resulting in fragmentation if sufficient energy is deposited. The secular frequency of motion of the product ions are not in resonance with the supplemental RF signal and the ions are therefore 'cooled' by collisions with the background gas to the center of the trap. It is possible, however, for ion ejection to occur prior to fragmentation. The Dehmelt pseudopotential well associated with ion storage in the ion trap is given by the equation

$$\overline{D_z} = q_z \frac{V}{8} = \frac{zeV^2}{m(r_0^2 + 2z_0^2)\omega^2} \tag{10}$$

where $\overline{D_z}$ is the Dehmelt potential. This is illustrated in Figure 2.5, where the energy E_{RE} represents the energy that is required at a specified q value in order for an ion to be ejected due to resonant excitation. Dissociation is typically performed at a q value of 0.25 to maintain a balance between the requirement for obtaining efficient ion fragmentation (rather than ejection), while keeping an appropriate low mass cutoff value for storage of the resultant product ions.

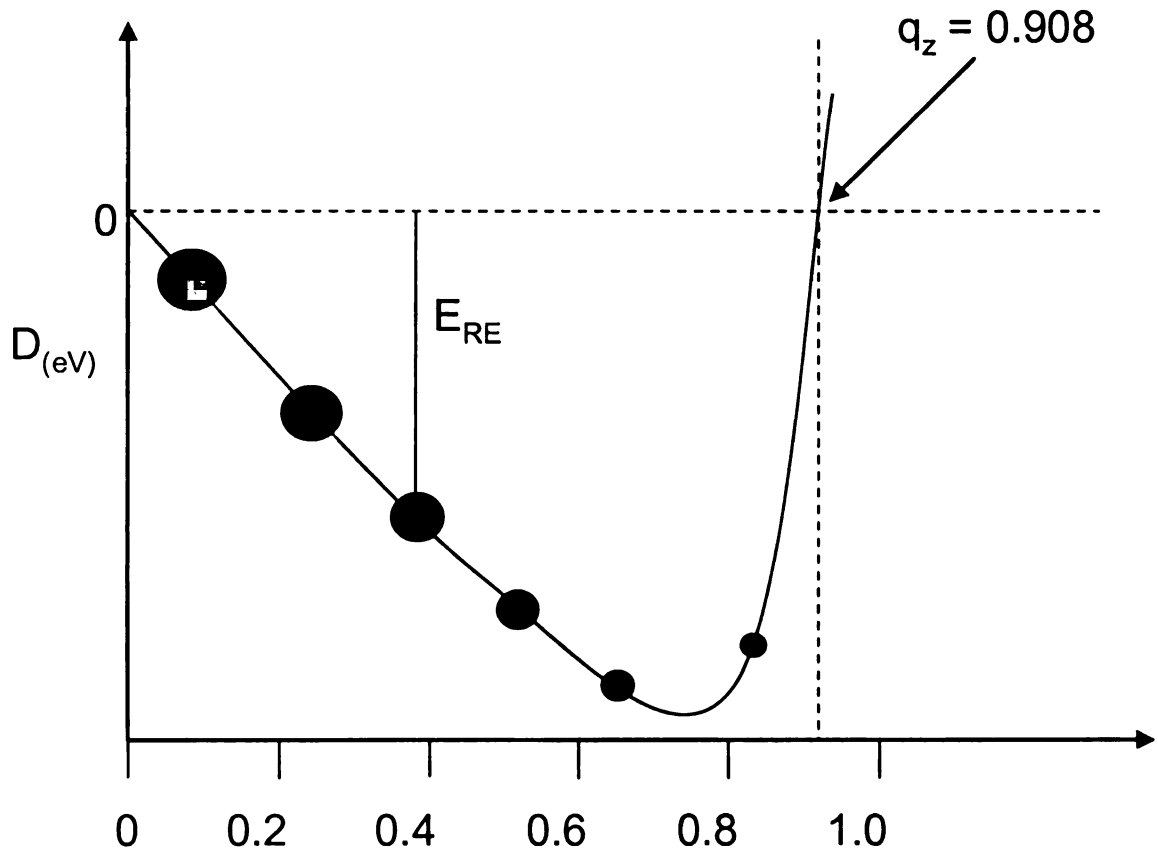

Figure 2.5 Dehmelt pseudo well potential D (eV) as a function q_z. Higher mass ions for a given V value have lower Dehmelt trapping energies. (Reproduced and modified from reference 42)

2.1.3 Detectors

The remaining components of the mass spectrometer are the detector and a data system. The detector converts the ion flux into a proportional electric current. One of the most common detectors is a continuous-dynode electron multiplier with a conversion dynode (Figure 2.6).

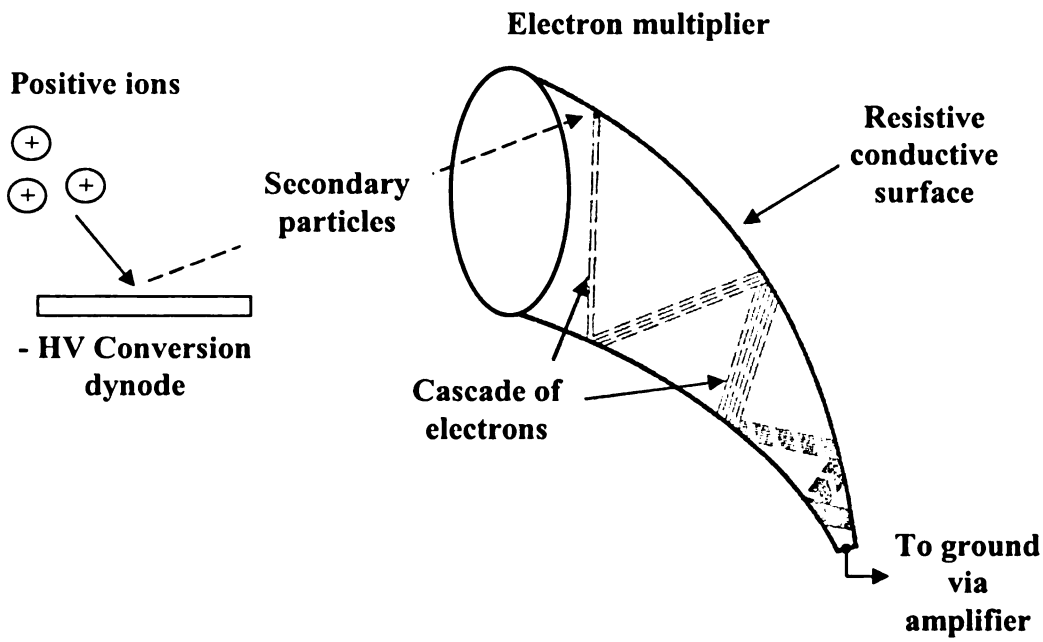

Figure 2.6 Diagram of a continuous-dynode electron multiplier with a conversion dynode. (Reproduced and modified from reference 45)

When an ion strikes the conversion dynode, secondary particles (negative ions and electrons for positive ions) are emitted and accelerated into the electron multiplier where they strike the surface of the electron multiplier with enough force to cause secondary electrons to be ejected. Drawn towards the ground potential at the end of the multiplier, the emitted secondary electrons move further into the electron multiplier. As they do so, they too strike the surface of the multiplier causing the emission of more and more

electrons (cascade effect), thus amplifying the original signal. The data system then records the magnitude of this electrical signal from the detector as a function of mass-to-charge (*i.e.*, a mass spectrum).

CHAPTER THREE

Experimental

3.1 Materials

Methanol (HPLC grade), 1,3-dimethyl-1,3-diphenylurea (methyl centralite, MC), 1,3-diethyl-1,3-diphenylurea (ethyl centralite, EC), and diphenylamine (DPA) were purchased from Sigma-Aldrich (St. Louis, MO, USA). Deionized water was purified by a Barnstead nanopure diamond purification system (Dubuque, Iowa, USA). All reagents were used as supplied without further purification. Men's short sleeve white t-shirts by Fruit of the Loom (100% cotton, size XXL) were obtained from a local retail store.

Smokeless powder samples were obtained by removing the powder from the following cartridges: (1) 9 mm, 124 grain, full metal jacket (FMJ) by Federal, (2) 9 mm +P, 135 grain, jacketed hollow point (JHP) by Federal, (3) 0.45 automatic colt pistol (ACP), 230 grain, JHP by Federal, (4) 0.45 ACP, 230 grain, FMJ by Federal, (5) 0.40 Smith and Wesson (S&W), 155 grain, JHP by Federal, (6) 0.40 S&W, 155 grain, JHP ('Silvertip') by Winchester, and (7) 0.357 Magnum, 125 grain, semi-jacketed hollow point by Remington-Peters. Cartridges 1, 3, 4, and 5 were provided by the Michigan State University Police Department, while cartridges 2, 6, and 7 were personally provided by a certified firearm instructor employed by the Michigan State University Police Department. All cartridges were stored in a cool, dry location prior to use.

Gunshot residue samples were obtained by firing the aforementioned cartridges from the following handguns: (1) Glock Model 19, 9 mm, 4″ barrel (for cartridges 1 and 2), (2) Sigarms Model P220, .45 ACP (for cartridges 3 and 4), (3) Sigarms Model P229,

4″ barrel (for cartridges 5 and 6), and (4) Smith and Wesson Model 66, 2.5″ barrel (for cartridge 7). The Sigarms Model P229 firearm was owned by the Michigan State University Police Department. All other firearms, and the MPro7 cleaning system (bore cleaning gel and gun cleaner) that was used, were personally owned by a certified firearm instructor employed by the Michigan State University Police Department.

3.2 Standard Solutions of the Smokeless Powder Stabilizers MC, EC, and DPA for Analysis by Mass Spectrometry

MC was dissolved in methanol to make a stock solution of 100 pmol/μL. This solution was stored in a -20 °C freezer and dilutions with methanol were made daily to obtain concentrations of ~ 0.000001, 0.00001, 0.0001, 0.001, 0.01, 0.1, 1, and 10 pmol/μL. This process was repeated for EC and DPA. All solutions were centrifuged prior to injection into the mass spectrometer

3.3 Smokeless Powder Samples

3.3.1 Stereomicroscopy of Smokeless Powder Samples

A Nikon SMZ800 stereomicroscope equipped with a Nikon digital DXM1200F camera was used to photograph the smokeless powders (Nikon Corporation, Tokyo, Japan). The software used was Nikon ACT-1, version 2.62. Direct lighting (used for the powders from cartridges 2, 4, and 7) was supplied by a Schott Fostec light (Schott North America Inc., Elmsford, NY), while oblique lighting (used for the powders from cartridges 1, 3, 5, and 6) was supplied by a standard light bulb. The photographs were

adjusted for contrast, color, and brightness using Adobe PhotoShop, version 8.0 (Adobe Systems Incorporated, San Jose, CA).

3.3.2 Extraction of Stabilizers from Smokeless Powder Samples for Analysis by Mass Spectrometry

1 mg of each smokeless powder was extracted with 1 mL of methanol by vortexing for about 30 seconds. The subsequent solutions were diluted to 0.1 mg/mL total concentration with methanol. In order to compare extraction efficiency, 10 mg of powder 2 (9 mm +P) was extracted with 10 mL of methanol by vortexing for roughly 30 seconds, yielding a solution with a total concentration of 0.1 mg/mL. All solutions were centrifuged prior to injection into the mass spectrometer.

5 mg of each smokeless powder was extracted with 1 mL of methanol by either (1) vortexing for approximately 30 seconds or (2) crushing with the end of a spatula for about 1 minute and then vortexing for about 10 seconds. The powder was weighed before and after extraction in order to determine and compare extraction yields. Dilutions were then performed with methanol to obtain solutions with the desired concentration of extracted material (0.02 mg/mL, 0.5 mg/mL, and 0.1 mg/mL). All solutions were centrifuged prior to injection into the mass spectrometer.

5 mg of each of the smokeless powders was extracted with 1 mL of deionized water by crushing with the end of a spatula for about 1 minute and then vortexing for about 10 seconds. No dilutions were made. All solutions were centrifuged prior to injection into the mass spectrometer.

3.4 Gunshot Residue (GSR)

3.4.1 Collection of GSR

Target paper was fastened to a foam target backer and 12″ x 12″ squares of cloth cut from white t-shirts were pinned to the paper one at a time to avoid the accidental deposition of gunshot residue on cloth not being fired at. Each cloth square was pinned to a different location on the target paper to avoid gunshot residue transferring from the target paper to the cloth. To avoid possible cross contamination between cartridges, the target paper was changed between each cartridge type and the firearms were extensively cleaned between cartridges.

Each cartridge was fired twice at a firing distance of 3″: once into a square of unwashed cloth and once into a square of cloth that had been extensively washed with deionized water to remove any potential contaminants and air dried. Cartridge 2 (9 mm +P) was also fired into a square of cloth that had been machine washed and dried. Once fired into, the square of cloth was placed between two pieces of wax paper, folded, and scaled in a plastic storage bag. This process was repeated at a firing distance of 12″. These distances were chosen because they are within the range of distances commonly used by forensic labs for test firings.

3.4.2 Extraction of GSR from Cloth for Analysis by Mass Spectrometry

A sample of cloth (~ ¼″ by ¼″) was cut from directly beside the bullet hole where visible gunshot residue was present. This cloth was placed in 1 mL of methanol and vortexed for approximately 30 seconds. No dilutions were made and all solutions were

centrifuged prior to injection into the mass spectrometer. Samples were run on the day of collection.

3.5 Mass Spectrometry

All experiments were performed using a Thermo model LCQ quadrupole ion trap mass spectrometer (Thermo Scientific, San Jose, CA). Solutions were introduced to the mass spectrometer at a flow rate of 1 μL/min by nanoelectrospray ionization (nESI). The nESI conditions were optimized to maximize the intensity of the protonated precursor ion and to minimize the appearance of in-source fragmentation peaks. Typical nESI conditions were: spray voltage 2.5 kV, heated capillary temperature 125 °C, capillary voltage 0 V, and tube lens voltage 0 V. Mass spectra were acquired using the normal resonance ejection scan mode of the quadrupole ion trap mass spectrometer. The precursor ion accumulation time for each scan was controlled by the automatic gain control (AGC) function of the instrument in order to maintain an ion target number of 2×10^7 (arbitrary value). CID MS/MS and MS^3 spectra were acquired at an activation q value of 0.25 using isolation widths of 3-10 Da, normalized collision energies of 10 - 50%, and an activation time of 30 ms or 300 ms. The values were chosen such that the gentlest conditions were used in order to completely dissociate the selected precursor ion (*i.e.*, some precursor ions required a larger normalized collision energy and/or longer activation time). Full and selected reaction monitoring (SRM) scan types were used. The MS spectra and the MS/MS and MS^3 product ion spectra shown throughout this thesis are an average of 100 and 60 individual mass analysis scans, respectively.

CHAPTER FOUR

Nanoelectrospray Ionization Tandem Mass Spectrometry for the Analysis and Identification of Ethyl Centralite, Methyl Centralite, and Diphenylamine

4.1 Introduction

Smokeless powder is one of the most common explosives used today in gunpowder and improvised explosive devices (IEDs). The ability to rapidly identify and characterize smokeless powder samples and their residues is therefore of great forensic value. The most common method for the forensic analysis of smokeless gunpowder or gunshot residue is to identify inorganic components contained in the primer [8, 12]. With the relatively recent introduction of heavy metal-free primers, however, there is the need for the development of a different approach, such as the analysis of organic components in the propellant [12, 22]. Stabilizers, added to slow the decomposition of nitrocellulose, are considered to be the most unique organic components of smokeless powder [15, 28, 29]. The three most commonly used stabilizers are methyl centralite (MC, Structure 1), ethyl centralite (EC, Structure 2), and diphenylamine (DPA, Structure 3).

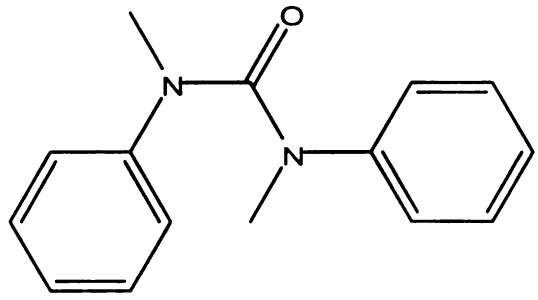

Structure 1: Methyl Centralite (MC)

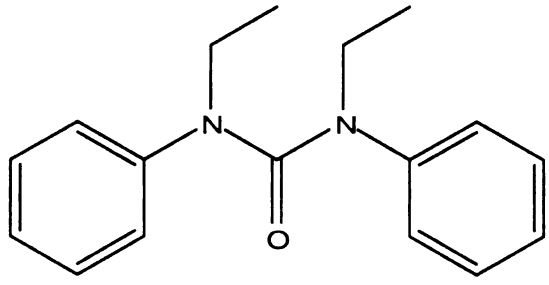

Structure 2: Ethyl centralite (EC)

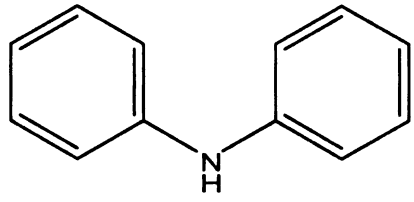

Structure 3: Diphenylamine (DPA)

As discussed in Section 1.5 there have been many techniques used to analyze smokeless powder, but mass spectrometry offers the much desired sensitivity and specificity. The quadrupole ion trap mass spectrometer is an ideal instrument due to its ability to perform multiple stages of dissociation (*e.g.*, MS^3), thus allowing further characterization and possible identification of unknown components. Although mass spectrometry is commonly coupled with either gas chromatography (GC) or liquid chromatography (LC), GC can cause the thermal degradation of some compounds, such as DPA, while LC is limited due to the potentially wide range of polarities present in a powder. Nanoelectrospray ionization (nESI), however, helps overcome these difficulties and minimizes analysis time by allowing direct introduction of the sample to the mass spectrometer. In this study, standard solutions of the organic stabilizers commonly found

in smokeless powder (MC, EC, and DPA) were examined by nESI-MS using a quadrupole ion trap in order to develop and optimize a method for the routine detection and compositional analysis of smokeless powder.

4.2 Development and Optimization of Conditions for the Detection of MC, EC, and DPA

It is important to maximize the signal for the ions of interest in order to achieve a low limit of detection (LOD). This is especially true for residues of smokeless powder, which are more likely to contain only trace amounts of the stabilizers compared to the amounts in unburned powder. The conditions needed to maximize the signal from one stabilizer, however, may cause the signals from the other stabilizers to decrease. It is therefore crucial that the instrumental conditions be optimized for the simultaneous identification of all three stabilizers, since it would not be known at first which, if any, stabilizer was present in a sample. Thus, a compromise must be reached whereby the conditions used maximize the signals obtained from MC, EC, and DPA such that all have a signal high enough for trace analysis.

Typical nESI-MS conditions were optimized to maximize the intensity of the protonated MC, EC, and DPA ions, while minimizing the appearance of in-source fragmentation peaks. In-source fragmentation, or source-collision induced dissociation, occurs when sufficient kinetic energy is imparted to an ion while in the source to cause the ion to fragment when it collides with solvent or air molecules. This type of fragmentation can reduce the intensity of the signal from the precursor ion, in this case MC, EC, or DPA, which can hinder detection and identification if the compounds are

only present in trace amounts. Most of the nESI-MS conditions (*i.e.*, the entrance lens, interoctapole lens, multipole 1 and 2 etc.) did not greatly affect the peaks observed, so standard settings were used without problems. The capillary voltage, tube lens voltage, and heated capillary temperature, however, were found to have a significant affect on the abundance of the protonated precursor ion and on the extent of in-source fragmentation. The capillary voltage was examined from 0 V to -60 V and the effects of the tube lens voltage were analyzed from 0 V to -250 V. At the higher voltages for both the capillary and the tube lens, in-source fragmentation became pronounced. The heated capillary temperature was examined from 100 °C up to 325 °C. If the temperature was set too low, the signal was lost, but if the temperature was too high, in-source fragmentation occurred. For these reasons, the capillary and tube lens voltages were set at 0 V and the heated capillary temperature was set at 125 °C for all three compounds of interest.

4.3 Analysis of the Mass Spectra Obtained for MC, EC, and DPA Standards

Once the nESI-MS conditions were optimized, spectra for MC, EC, and DPA could be obtained under these conditions. In a forensic context, an analyst will not be able to spend a lot of time on the analysis of any given sample. It is therefore necessary for a forensic scientist to be able to specifically look for peaks in a spectrum that are known to be associated with one of these stabilizers instead of having to analyze an entire spectrum. Tandem mass spectrometry can then be used to conclusively identify peaks of interest, if the fragmentation pathway has been previously established with standards. Thus, by running standards of MC, EC, and DPA, key peaks and their dissociation behavior can be established such that unknown powders can later be rapidly analyzed.

Figure 4.1 shows the mass spectra acquired for MC (Figure 4.1A), EC (Figure 4.1B), and DPA (Figure 4.1C) under optimized conditions. MC and EC were analyzed at concentrations of 10 pmol/μL, while DPA was run at 100 pmol/μL. DPA did not ionize as efficiently as MC and EC and thus required a higher concentration in order to achieve a signal-to-noise (S/N) ratio comparable to that of MC and EC. Even at the 100 pmol/μL concentration, however, the spectrum for DPA (Figure 4.1C) is noisier than the others, but DPA could not be run more concentrated without contaminating the system. DPA is therefore likely to have a higher limit of detection than that of MC and EC. At these high concentrations (10 pmol/μL for MC and EC, 100 pmol/μL for DPA), MC and EC form dimers and adducts with Na and K, while DPA forms a dimer, trimer, and quadramer and Na adducts, but the S/N ratio is such that background ions are minimized and the minimal in-source fragmentation obtained under the optimized conditions is easily observed. A good S/N ratio is initially required in order to clearly identify peaks in the spectra of the standards. Once peaks of interest are identified, however, high background ions would be inconsequential in a forensic setting as long as the ion of interest could be detected.

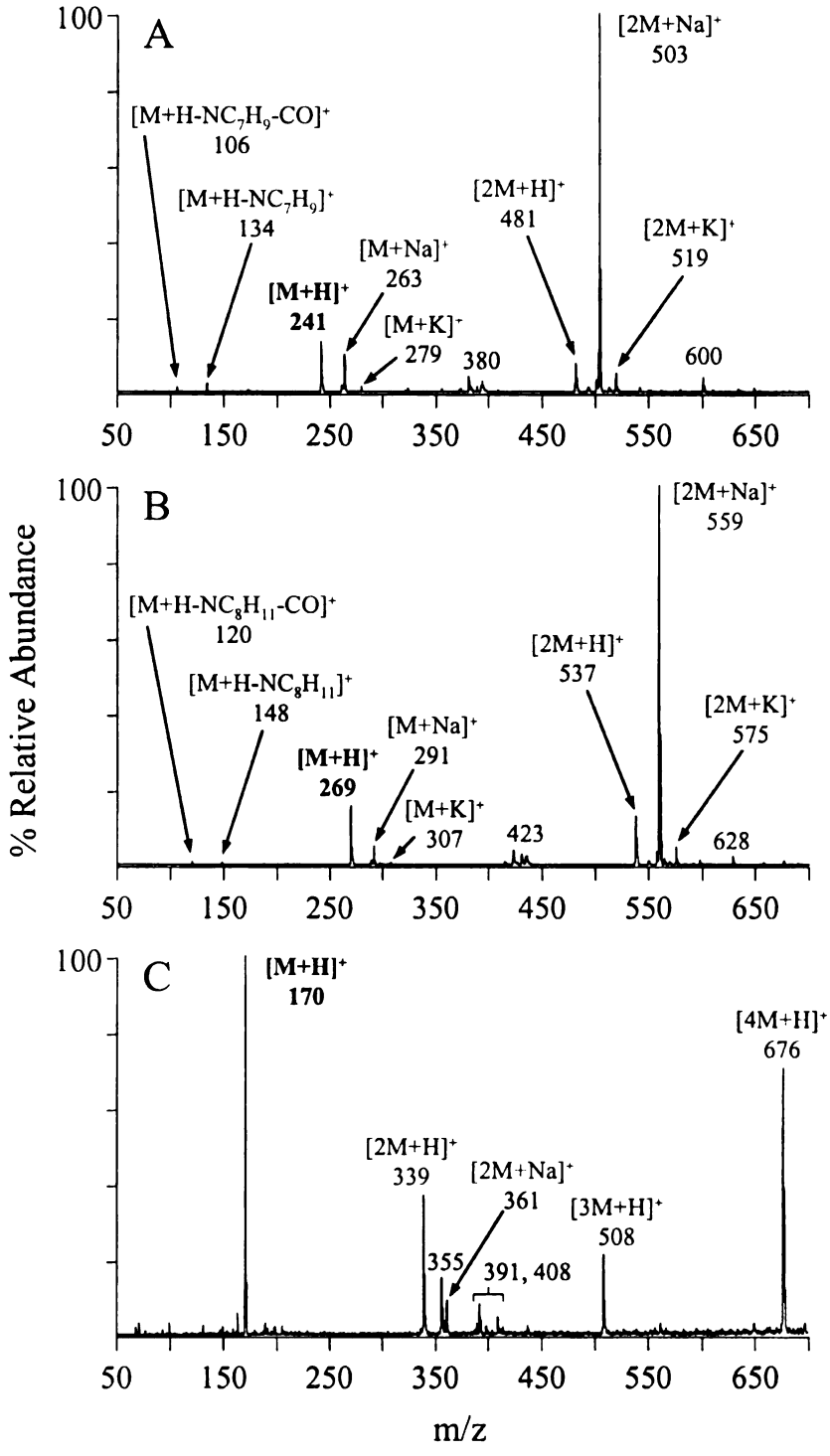

Figure 4.1 Mass spectra under optimized nESI-MS conditions for standard solutions of (A) MC at 10 pmol/μL, (B) EC at 10 pmol/μL, and (C) DPA at 100 pmol/μL.

4.3.1 MC

Tandem mass spectrometry was used to identify and characterize the peaks in the spectra obtained for MC (Figure 4.1A) and this data is shown in Table 4.1 below. Dissociation of the protonated precursor ion for MC (m/z 241 in Figure 4.1A) yielded a product ion at m/z 134, corresponding to $[NC_7H_8CO]^+$, and a product ion at m/z 106, which could be the ion $[NC_7H_8]^+$, produced by the loss of CO from the product ion at m/z 134. This was confirmed by performing MS^3 on the m/z 134 product ion, which yielded the ion at m/z 106. The mechanistic pathway is shown in Scheme 4.1. The ion at m/z 481 has a mass consistent with the protonated MC dimer. When MS/MS was performed on this precursor ion, the product ion formed was at m/z 241, the same m/z as protonated MC. MS^3 on this m/z 241 product ion resulted in the formation of ions at m/z 106 and 134, confirming that the product ion at m/z 241 is $[MC+H]^+$ and the precursor ion at m/z 481 is $[2MC+H]^+$.

While the ions at m/z 263 and 279 did not readily dissociate, the mass difference between these ions and the $[MC+H]^+$ ion at m/z 241 is 22 and 38, respectively. These characteristic mass differences are indicative that the ion at m/z 263 is the sodium adduct $[MC+Na]^+$, while the ion at m/z 279 is the potassium adduct $[MC+K]^+$. This same logic holds for the ions at m/z 503 and 519, which have masses that are consistent with Na and K adducts for the MC dimer, respectively. Further evidence of this is obtained through MS/MS experiments, whereby the ion at m/z 503 (probable $[2MC+Na]^+$ ion) fragments to give m/z 263 (the m/z of the likely $[MC+Na]^+$ adduct) and the ion at m/z 519 (probable $[2MC+K]^+$ ion) fragments to yield m/z 279 (the m/z of the $[MC+K]^+$ adduct). The ion at m/z 600 dissociates to yield product ions at m/z 263, 320, 360, and 429, none of which

would fragment further to give MS^3 data. The product ion at m/z 263, however, could be the adduct $[MC+Na]^+$, thus the ion at m/z 600 could be a complex containing MC and a Na adduct.

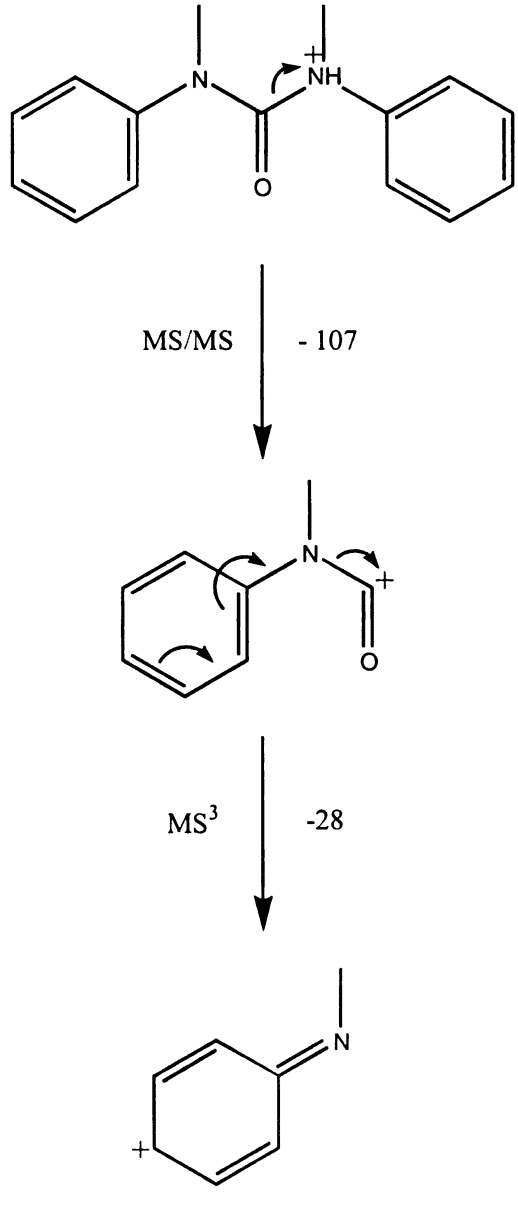

Scheme 4.1 Possible mechanism for the fragmentation of protonated MC (m/z 241) to form product ions at m/z 134 and 106.

The other ions seen in the mass spectra for MC either did not fragment due to low abundance, such that characterization was not possible, or their fragmentation behavior did not readily lead to identification as there were no characteristic losses. Some of these ions could be tentatively identified based on comparisons between the MC and EC spectra (discussed in section 4.3.2) All of these ions, however, have low relative abundances compared to the main MC peaks, which would be the peaks of interest in a forensic analysis aimed at identifying an unknown as smokeless powder, since MC, EC, and DPA are the organic components considered most characteristic of smokeless powder.

Table 4.1 MS and MS^n data obtained by nESI quadrupole ion trap mass spectrometry for a 10 pmol/μL standard solution of MC in methanol.

Component	**Precursor ions (m/z)**	**MS/MS product ions (m/z) (% relative abundance)**	**MS^3 product ions (m/z) (% relative abundance)**
MC	241	106 (4%) 134 (100%)	106 (100%)
MC+Na	263		
MC+K	279		
Unidentified	380	260 (100%)	216 (100%)
2MC	481	241 (100%)	106 (1%) 134 (100%)
*MC	493		
*MC	500		
2MC+Na	503	263 (100%)	
2MC+K	519	279 (100%)	
*MC	600	263 (94%) 320 (86%) 360 (100%) 429 (30%)	

* Unidentified MC complex/adduct

4.3.2 EC

The fragmentation behavior of EC is similar to that seen for MC due to their similar structures (Structures 2 and 1, respectively). The MS and MS^n data for EC is summarized in Table 4.2 below. The protonated precursor ion at m/z 269 (Figure 4.1B) dissociates to give product ions at m/z 148 and 120. The product ion at m/z 148 is likely the ion $[NC_8H_{10}CO]^+$, while the ion m/z 120 would be $[NC_8H_{10}]^+$, formed by the loss of CO from the m/z 148 product ion. As expected, MS^3 of the m/z 148 product ion gave the ion at m/z 120. MS^4 of the ion at m/z 120 yielded an ion at m/z 92, or $[NC_6H_6]^+$ formed by the loss of CH_2CH_2. This is illustrated mechanistically in Scheme 4.2.

The ion at m/z 537 has a mass that is consistent with the protonated EC dimer. MS/MS of m/z 537 gave the product ion m/z 269, which could be $[EC+H]^+$. MS^3 of this product ion at m/z 269 yielded ions at m/z 148 and 120 confirming that the product ion at m/z 269 is $[EC+H]^+$ and that the precursor ion at m/z 537 is $[2EC+H]^+$. The mass difference between the $[EC+H]^+$ ion at m/z 269 and the ions at m/z 291 and 307 was 22 and 38, respectively indicating that the ion at m/z 291 is the sodium adduct $[EC+Na]^+$, while the ion at m/z 307 is the potassium adduct $[EC+K]^+$. Similarly, the ions at m/z 559 and 575 have masses and fragmentation behavior consistent with $[2EC+Na]^+$ and $[2EC+K]^+$, respectively.

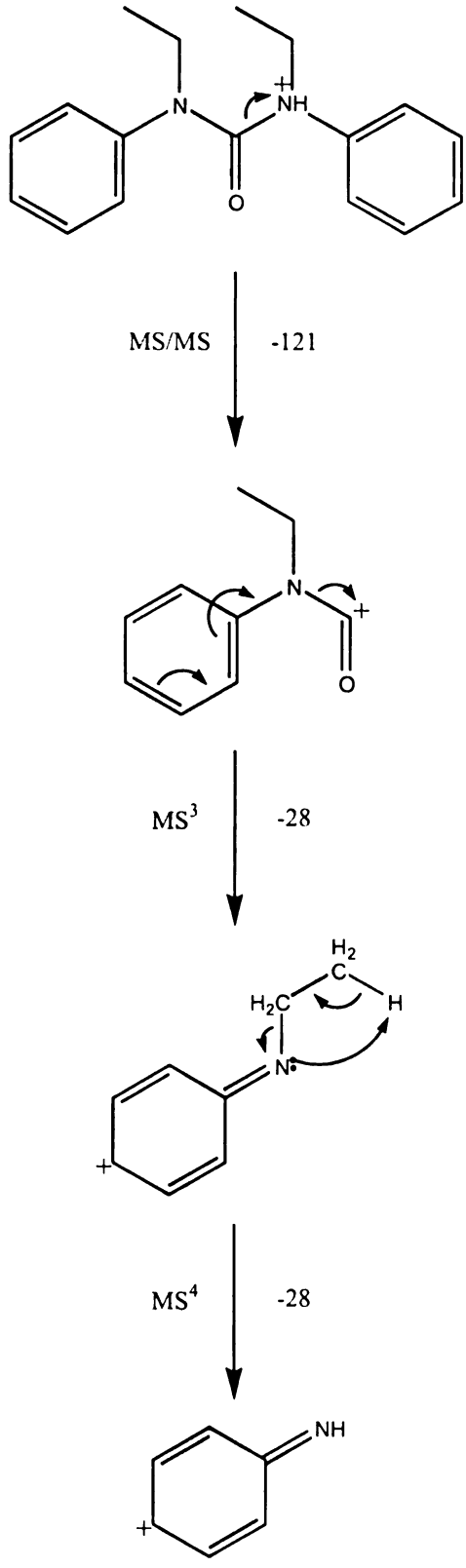

Scheme 4.2 Possible mechanism for the fragmentation of protonated EC (m/z 269) to form product ions at m/z 148, 120, and 92.

The ion at m/z 628 fragmented to give five product ions that included m/z 269 and m/z 291, which could be $[EC+H]^+$ and $[EC+Na]^+$, respectively. MS^3 of the product ion at m/z 269 yielded fragmentation that is consistent with $[EC+H]^+$. The product ion at m/z 291, however, did not fragment, but this would be consistent with observations for the $[EC+Na]^+$ ion. As was the case of the ion at m/z 291, none of the other three product ions would fragment and thus further characterization of the ion at m/z 628 was limited. The data from the ions at m/z 269 and 291, however, provide strong evidence that the ion at m/z 628 is a complex containing EC and a Na adduct. This also provides further evidence that the ion observed at m/z 600 for MC (Figure 4.1A) is indeed an MC and Na containing complex as proposed because the mass difference between the EC ion at m/z 628 and the MC ion at m/z 600 is 28, or the mass difference between MC and EC (mass of 28 = C_2H_4). This mass difference of 28 is seen for EC and MC monomers identical in composition except that one contains EC and one contains MC (such as $[EC+H]^+$ at m/z 269 and $[MC+H]^+$ at m/z 241 or $[EC+Na]^+$ at m/z 291 and $[MC+Na]^+$ at m/z 263).

The ions at m/z 549 and 556 in the EC spectrum have a mass difference between them and the ions at m/z 493 and 500 seen in the MC spectra of 56, or the mass difference between 2MC and 2EC (mass of 56 = C_4H_8). This difference is seen for other ions such as $[2EC+Na]^+$ at m/z 559 and $[2MC+Na]^+$ at m/z 503. This suggests these ions may have identical compositions except that the ions at m/z 549 and 556 contain the EC dimer and the ions at m/z 493 and 500 contain the MC dimer. This is further confirmed by comparing the mass of these ions with the respective protonated monomer. The ions at m/z 549 and 556 in the EC spectrum have a mass difference between them and the $[EC+H]^+$ ion (m/z 269) of 280 and 287, respectively. The mass difference for the ions at

m/z 493 and 500 seen in the MC spectra are 252 and 259 when compared to the $[MC+H]^+$ ion (m/z 241). The difference between 280 and 252 and the difference between 287 and 259 is 28, the mass difference between MC and EC. As was the case for EC, though, these unidentified ions are low in abundance and therefore of little forensic value compared to the other identified peaks.

m/z 493 and 500 seen in the MC spectra are 252 and 259 when compared to the $[MC+H]^+$ ion (m/z 241). The difference between 280 and 252 and the difference between 287 and 259 is 28, the mass difference between MC and EC. As was the case for EC, though, these unidentified ions are low in abundance and therefore of little forensic value compared to the other identified peaks.

Table 4.2 MS and MS^n data obtained by nESI quadrupole ion trap mass spectrometry for a 10 pmol/μL standard solution of EC in methanol.

Component	**Precursor ions (m/z)**	**MS/MS product ions (m/z) (% relative abundance)**	**MS^3 product ions (m/z) (% relative abundance)**	**MS^4 product ions (m/z) (% relative abundance)**
EC	269	120 (14%) 148 (100%)	120 (100%)	92 (100%)
EC+Na	291			
EC+K	307			
Unidentified	423	288 (100%)	181 (70%) 223 (98%) 274 (100%)	
2EC	537	269 (100%)	120 (9%) 148 (100%)	
*EC	549	414 (100%) 423 (40%)	280 (12%) 289 (65%) 298 (100%)	
*EC	556			
2EC+Na	559	291 (100%)		
2EC+K	575	307 (100%)		
*EC	628	269 (15%) 291 (100%) 360 (82%) 434 (55%) 457 (32%)	120 (7%) 148 (100%)	120 (100%)

* Unidentified EC complex/adduct

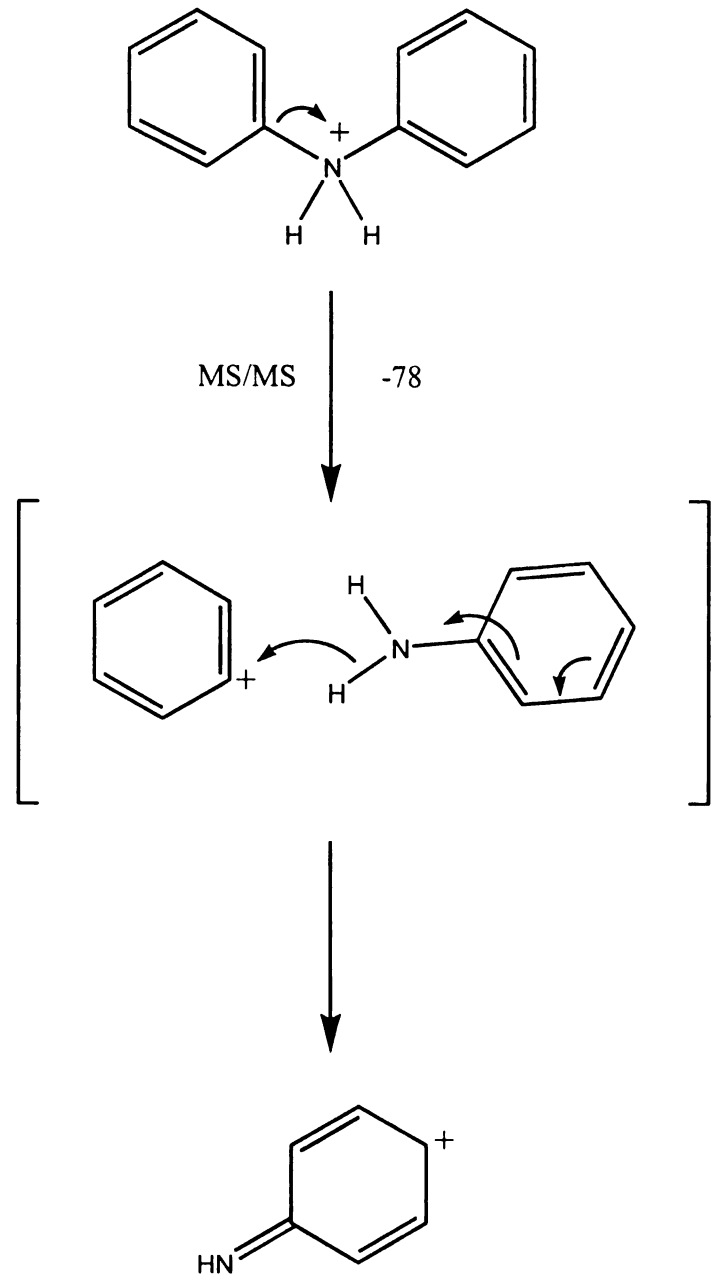

Scheme 4.3 Possible mechanism for the fragmentation of protonated DPA (m/z 170) to form a product ion at m/z 92.

Table 4.3 MS and MS^n data obtained by nESI quadrupole ion trap mass spectrometry for a 100 pmol/μL standard solution of DPA in methanol.

Component	Precursor ions (m/z)	MS/MS product ions (m/z) (% relative abundance)	MS^3 product ions (m/z) (% relative abundance)
DPA	170	92 (100%)	
2DPA	339	170 (3%) 303 (52%) 321 (100%)	92 (100%) 303 (100%)
Unidentified	355	339 (100%)	
2DPA+Na	361		
Unidentified	391	296 (100%)	
Unidentified	408	221 (100%) 249 (88%) 266 (32%) 294 (32%) 362 (23%)	80 (100%)
3DPA	508	170 (4%) 339 (100%)	92 (100%)
4DPA	676	339 (100%)	170 (100%)

4.4 Limits of Detection and Calibration Curves

In order to determine the limit of detection (LOD) and create calibration curves for MC, EC, and DPA, each standard was run at concentrations ranging from 0.000001 pmol/μL to 10 pmol/μL. Selected reaction monitoring (SRM) was used to help determine the LOD as this is an ideal scan type for trace analysis. As the name suggests, SRM monitors a specific reaction, such as a specific fragmentation pathway for a given ion. First, the parent ion is trapped in the mass analyzer and all other ions are ejected. The selected precursor ion is then fragmented into its product ions. The product ion of

interest is ejected from the mass analyzer to produce an SRM product ion mass spectrum. Data is not collected for any of the other precursor or product ions. The advantages of SRM compared to the full scan mode are that it allows for the rapid analysis of trace components in a complex mixture by improving S/N and detection limits.

In this work, at low concentrations the protonated precursor ions were sufficiently low in abundance as to be in the noise. As the fragmentation behavior of these ions, however, was previously determined (Section 4.3), SRM could be used to monitor the most abundant product ion produced by the dissociation of the $[M+H]^+$ ion. For MC this product ion was m/z 134. Similarly, the product ion at m/z 148 was monitored for EC and the product ion at m/z 92 was used for DPA. Using this method, the LOD for MC and EC was found to be 0.001 pmol/μL, while the LOD for DPA was found to be 0.01 pmol/μL. The slightly higher LOD for DPA is consistent with its ionization efficiency being less than that of MC and EC, as mentioned in Section 4.2. While these LOD are very good, they could be improved further by using a linear two dimensional (2D) ion trap, which has improved sensitivity. This is because linear 2D quadrupole ion traps exhibit higher acceptance (*i.e.*, more efficient ion injection) compared to 3D traps, due to the lack of a quadrupolar field along the z-axis. 2D traps also have orders of magnitude greater ion storage capacity due to the larger volume of the device and the fact that ions are focused along the entire length of the quadrupole due to the radial nature of the quadrupolar confinement field [47, 48].

For each of the stabilizers, calibration curves were generated that ranged from the LOD for each standard up to 1 pmol/μL. As an example, Figure 4.2 shows the calibration curve for EC in methanol.

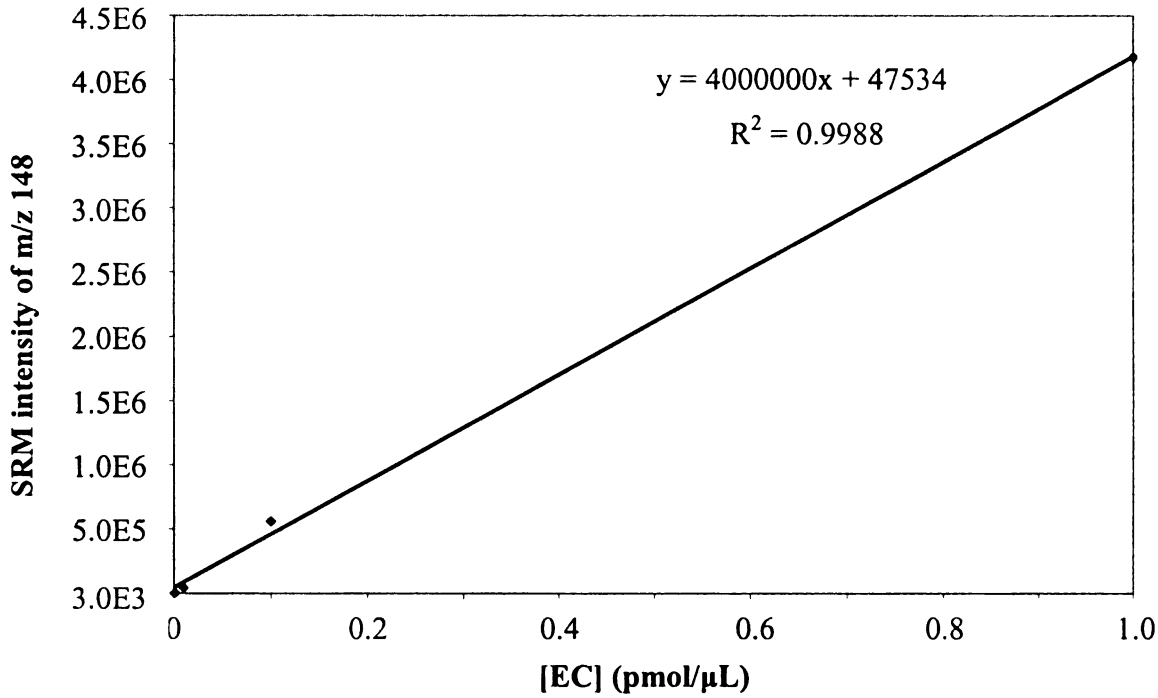

Figure 4.2 Calibration curve for EC in methanol (0.001 pmol/µL to 1 pmol/µL) using selected reaction monitoring of m/z 269 fragmenting to m/z 148.

The results from the standard solutions at 10 pmol/µL were not included in the calibration curves because at such high concentrations adducts and other complexes formed (Figure 4.1) to the point of causing the relative abundances of the $[MC+H]^+$, $[EC+H]^+$, and $[DPA+H]^+$ ions to decrease. Thus, adduct and complex formation makes quantification above the 1 pmol/µL concentration difficult. Also, the adduct ions are themselves not reliable candidates for quantification because of the widespread existence of Na and K that would greatly influence the concentration of these adducts. Even a simple change in the tubing of the nESI source could cause a drastic change in the abundance of these adducts as the new tubing may have very different concentrations of Na and K compared to the old tubing.

The calibration curves were also slightly non-linear at the lower concentrations. Thus quantification is not reliable without plotting a significantly large number of points at low concentrations to account for the non-linearity. Overall, due to the formation of complexes and adducts at high concentrations and non-linearity at low concentrations, quantification using nESI-MS is not reasonable. Although it may be possible to quantify using an internal standard or isotopic labeling, from a forensic standpoint, quantification of the components of smokeless powder is not as important as identification of the components. Hence, qualitative analysis is sufficient to identify a powder or residue as being smokeless powder and to differentiate between smokeless powders and their residues.

4.5 Summary

Standard solutions of the organic stabilizers MC, EC, and DPA, which are commonly found in smokeless powder, were examined by tandem mass spectrometry (MS/MS and MS^3) in a quadrupole ion trap using nESI in order to develop a method for the routine and rapid identification and comparison of smokeless powders. Following optimization of the ionization and mass analyzer conditions, mass spectra for standard solutions of MC, EC, and DPA were obtained. MC gave the characteristic fragmentation pathway m/z 241 → 134 → 106. EC's protonated precursor ion at m/z 269 dissociated to give 148 → 120 → 92. DPA fragmented from m/z 170 to m/z 92. This method was able to detect all three stabilizers using the same nESI-MS conditions. Acceptable LOD (0.001 pmol/μL, or 1 fmol/μL, for MC and EC and 0.01 pmol/μL, or 10 fmol/μL, for DPA) were obtained by utilizing the selected reaction monitoring (SRM) scan mode.

Calibration, however, was not possible due to non-linearity of the calibration curves at low concentrations and due to the formation of adducts (Na, K) and complexes at higher concentrations.

CHAPTER FIVE

Nanoelectrospray Ionization Tandem Mass Spectrometry for the Analysis of Smokeless Powder and its Residue

5.1 Introduction

While methyl centralite (MC), ethyl centralite (EC), and diphenylamine (DPA) are considered to be the most unique organic components in smokeless powders, they are used for other purposes. Methyl centralite (Structure 1) is found in celluloid and solid rocket propellant, as is ethyl centralite (Structure 2) [12, 16]. Diphenylamine (Structure 3) is used in rubber products and in the food industry. The nitrated derivatives of DPA that form as nitrocellulose degrades, however, are thought to be unique to smokeless powder as the other uses for DPA do not involve nitrating agents or processes [14, 29]. Thus, the identification of more than one of these stabilizers in a sample or identification of a nitrated DPA compound could provide more certainty that the substance being analyzed was smokeless powder, burned or unburned [16]. Previous experiments using mass spectrometry to analyze the organic stabilizers used in smokeless powder, however, have been limited in the number of stabilizers detected simultaneously or in the number of samples analyzed [28, 29].

In this study, samples of smokeless powder were obtained from seven different cartridges and assigned a number that will be used to refer to each powder: (1) 9 mm, 124 grain, full metal jacket (FMJ) by Federal, (2) 9 mm +P, 135 grain, jacketed hollow point (JHP) by Federal, (3) 0.45 automatic colt pistol (ACP), 230 grain, JHP by Federal, (4) 0.45 ACP, 230 grain, FMJ by Federal, (5) 0.40 Smith and Wesson (S&W), 155 grain,

JHP by Federal, (6) 0.40 S&W, 155 grain, JHP ('Silvertip') by Winchester, and (7) 0.357 Magnum, 125 grain, semi-jacketed hollow point by Remington-Peters. These powders were then compared based on their physical characteristics, *i.e.*, color, shape, texture, and size, and on their extraction characteristics. Finally, the smokeless powder samples and their residues were examined by using the previously optimized method for nESI-MS (Chapter 4) in a quadrupole ion trap.

5.2 Physical Characteristics of Smokeless Powder Samples

The initial characterization of unburned smokeless powder is typically a survey of the powder morphology using a stereomicroscope. If the powder morphologies are vastly different, the powders can be excluded as having originated from a common source. When the powders are not distinguished based on morphology, however, further chemical analyses are necessary. Figure 5.1 shows photographs taken of the seven powders used in this study using a stereomicroscope.

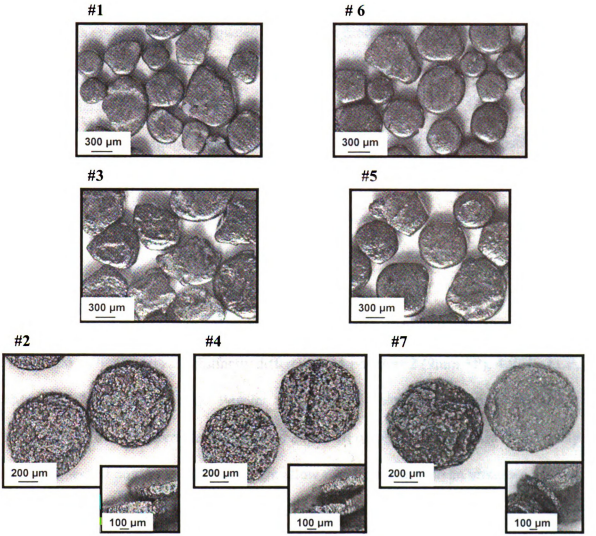

Figure 5.1 Stereomicroscopy photos of smokeless powder samples.

It can be seen than powders 1, 3, 5, and 6 have similar morphology. They are all relatively round in shape with slightly rough surfaces and a gray-brown color, almost like rocks or pebbles. Slight differences, however, can be seen among these four powders. Powder 3 is significantly rougher in texture than the other three powders, with the order of roughness (from most to least) being 3, 5, 6, and 1. Also, the color of powders 3 and 5

is somewhat different than it is for powders 1 and 6, which have a more brown hue to them. The sizes of particles in powders 1 and 6 are more widespread than for powders 3 and 5, with powders 1 and 6 have particles ranging from small (~ 300 μm) smooth spheres to large (~ 600 μm), circular-like shapes. Powders 3 and 5, however, have particles that are all roughly 600 μm. Powders 2, 4, and 7 consist of circular discs that are approximately 600 μm and grainy in texture. Powders 2 and 4 are dark gray in color, while powder 7 consists of some particles that are black and some that are light gray. The thickness of the particles for powders 2 and 7 is more variable than it is for powder 4.

Overall, powders 1 (9 mm), 3 (0.45 ACP, JHP), 5 (0.40 S&W, Federal) and 6 (0.40 S&W, Winchester) are distinctly different from powders 2 (9mm +P), 4 (0.45 ACP, FMJ), and 7 (0.357 Magnum). Powder 1, 3, 5, and 6 show enough similarities that it would be difficult to differentiate between them based on physical properties alone. Only the roughness of powder 3's surface might allow it to be matched to an unknown powder and for powders 1, 5, and 6 to be excluded. Powders 2 and 4 are also too similar in nature to be differentiated from one another based on physical appearance, but powder 7 can easily be identified because it is the only powder to contain particles of two different colors. Since only one of the seven powders could be definitively differentiated from the other powders, further analysis is needed.

5.3 Extraction Efficiency of Smokeless Powder Samples

As a rapid, initial survey of the extractability of smokeless powder in methanol, 1 mg of powder 2 (9 mm +P) was extracted with 1 mL of methanol by vortexing for about

30 seconds and diluted to 0.1 mg/mL concentration. 10 mg of this same powder was also extracted with 10 mL of methanol by vortexing for roughly 30 seconds, yielding a solution with a concentration of 0.1 mg/mL in methanol. The mass spectra for these solutions did not show any major differences in the ions seen or their abundances, indicating that similar amounts of the same material were being extracted with both methods. Thus, there is no need to use a large quantity of powder when extracting, which is significant in forensic cases since the amount of sample may be very limited.

In order to determine the mass of material extracted from the smokeless powders, 5 mg of each powder was extracted with 1 mL of methanol by vortexing for about 30 seconds. The supernatant solution was carefully pipetted off and the powder dried and reweighed in order to determine the amount of material extracted and allow calculation of an extraction yield. This same procedure was repeated for all the powders, but instead of simply vortexing the solutions, a spatula was used to thoroughly crush the powder and then the solution was vortexed for about 10 seconds. These methods were performed at least three times for each powder and the average extraction yields, along with relative standard deviations (RSDs), are given in Table 5.1. Also, 5 mg of each of the smokeless powders was extracted with 1 mL of deionized water using the crushing method. This was only done once for each powder, since it was clear that less material was being extracted into water than was extracted into methanol. Extraction yields for this solvent are also listed in Table 5.1.

Table 5.1 Extraction data for smokeless powder samples in methanol (MeOH) and in water (H_2O).

Powder	% Extracted in MeOH, Vortexed*	% RSD	% Extracted in MeOH, Crushed*	% RSD	% Extracted in H_2O, Crushed
1	6.03	34.60	12.05	6.67	8.68
2	43.06	14.53	53.52	4.29	5.21
3	20.63	14.48	20.05	2.00	4.67
4	40.24	13.50	39.50	6.68	6.26
5	3.19	33.30	25.27	1.73	7.05
6	7.52	10.52	12.48	11.85	10.75
7	37.45	13.09	46.34	7.15	10.38

* Average of 3 or more extractions.

The mass of extracted material for a given powder varied more when the solution was vortexed only versus when the powder was crushed first. This is evident in the RSDs for the two techniques as the RSDs for all the powders are higher when the powders were vortexed only, with the exception of powder 6 (0.40 S&W, Winchester) where the RSDs are about the same. Not only was there less variability in the amount of extracted material with the crushing technique, but more material was extracted for most of the powders – powders 3 (0.45 ACP, JHP) and 4 (0.45 ACP, FMJ) had essentially equivalent amounts of extracted material for both techniques.

While optimizing this extraction procedure, it became evident that this data could also be used to differentiate between samples of unburned smokeless powder as some trends were observed in the extraction data for the powders crushed in methanol.

Powders 1 (9 mm) and 6 (0.40 S&W, Winchester) had the least amount of material extracted (less than 15%), while powders 2 (9mm +P), 4 (0.45 ACP, FMJ), and 7 (0.357 Magnum) had over 40% extraction yields. Powders 3 (0.45 ACP, JHP) and 5 (0.40 S&W, Federal) yielded extractions of around 20-25%. This suggests that powders 2, 4, and 7 have the highest concentration of extractable organic components, while powder 1 and 6 have the least. The grouping of powders seen here is the same as the grouping based on similarities in physical characteristics (section 5.2). Thus, extractability can add another level of certainty when trying to determine if two powders are the same or different. Here, this would be especially useful for differentiating powders 3 and 5 from powder 1 and 6, which were difficult to distinguish based on physical traits.

5.4 Analysis of Smokeless Powder Samples by nESI-MS

The detection of the compounds MC, EC, and/or DPA in a powder or residue can provide strong evidence that the explosive used was smokeless powder. This can be used, for example, to determine the explosive used in a bombing or to look for gunshot residue surrounding a hole that is thought to be a bullet hole. Also, comparison of the presence or absence of these compounds in a powder can help distinguish it from other powders, especially when combined with differences in the powders' physical attributes and extraction yields.

For the seven powders used in this study, dilutions were performed in methanol on the solutions obtained by crushing in order to obtain concentrations of extracted material of 0.002 mg/mL, 0.02 mg/mL, 0.5 mg/mL, and 0.1 mg/mL. Mass spectra were

then collected using the previously optimized conditions (Section 4.2). The spectra obtained for powder 2 (9 mm +P) are shown in Figure 5.2 as an example.

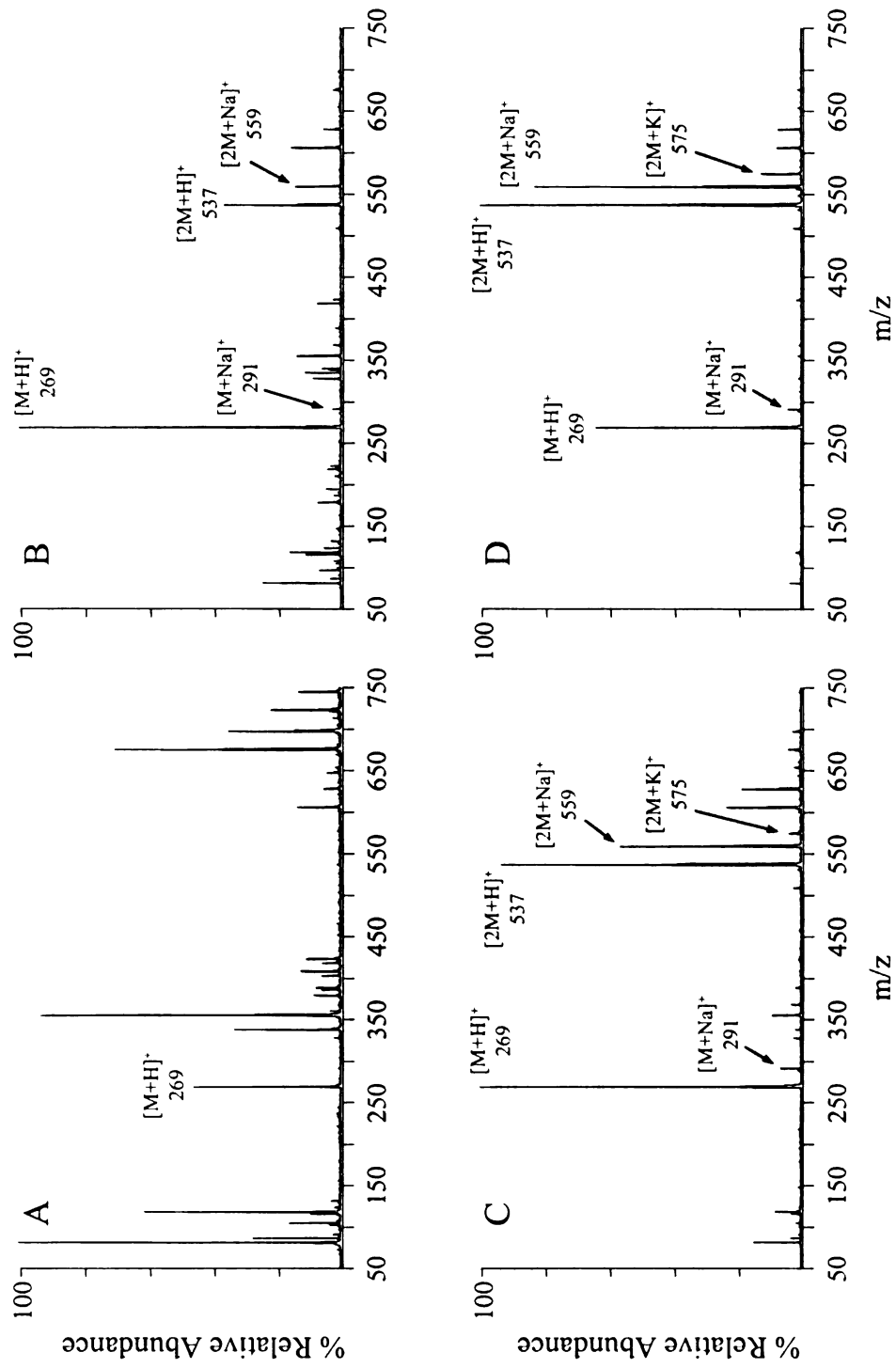

Figure 5.2 Mass spectra of smokeless powder 2 (9mm +P) in methanol at concentrations of (A) 0.002 mg/mL, (B) 0.02 mg/mL, (C) 0.05 mg/mL, and (D) 0.1 mg/mL extracted material.

At the lowest concentration (Figure 5.2A) there were no adducts or complexes, but the background is very high. As the concentration of extracted material was increased in order to overcome the background ions and thus improve S/N, the abundance of the adduct and dimer peaks also increased, showing that these compounds have a high tendency to form adducts and complexes. At the highest concentration (Figure 5.2D), the abundance of the adduct and dimer ions is significant, but the background is low, thus the S/N ratio is good. This trend was seen for all of the powders.

Figure 5.3 shows the spectra obtained for all the powders at the highest concentration of 0.1 mg/mL extracted material. Despite the peaks from adducts and complexes, these spectra eliminate much of the ambiguity over whether peaks are real (*i.e.*, from the powders' components) or whether they are background ions. It is important to be able to make this determination when analyzing unknown samples, as is typically the case with forensic evidence, so that any conclusions drawn are accurate and, for forensic cases, are able to provide admissible evidence for use in court proceedings.

Figure 5.3

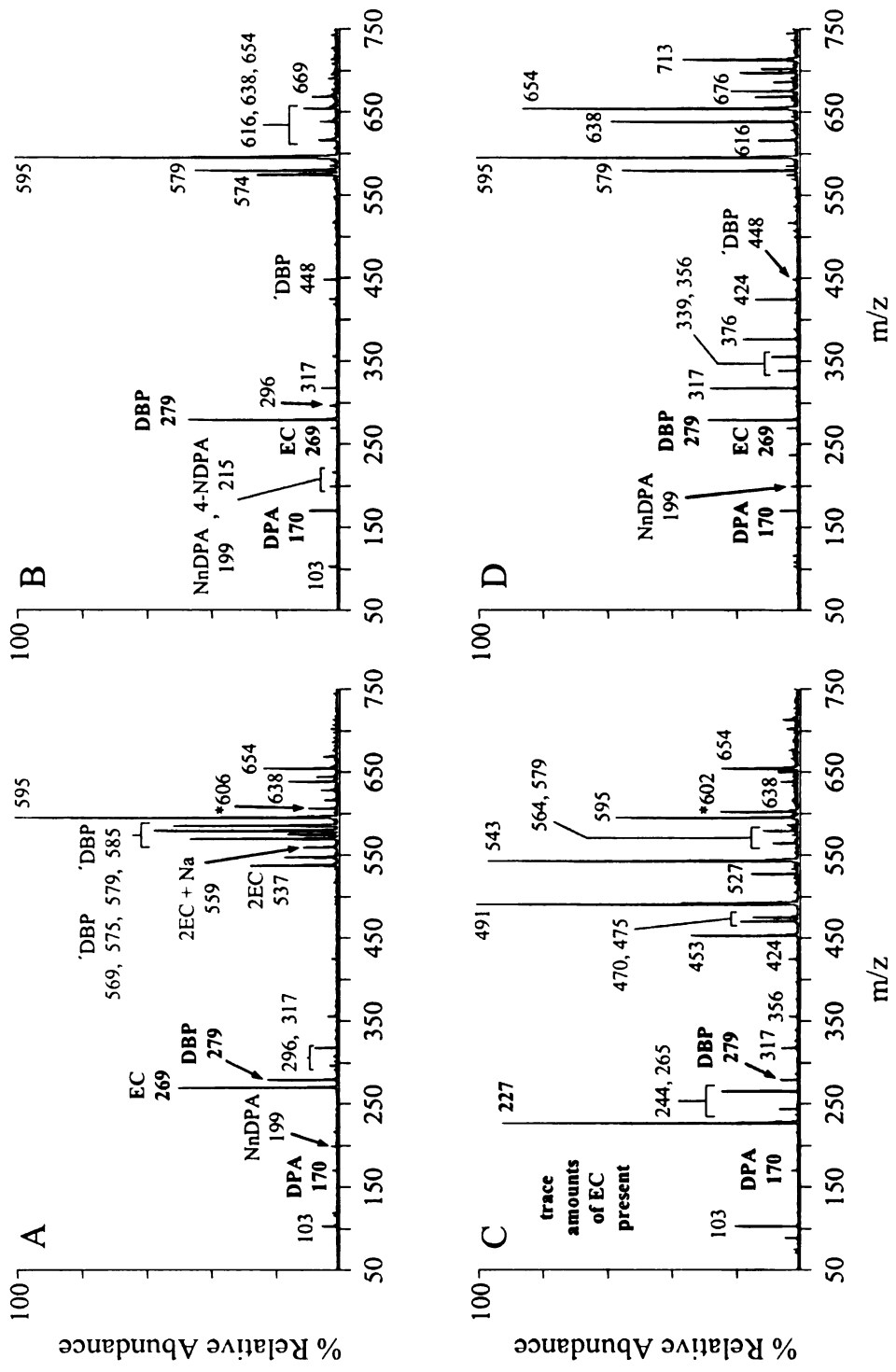
A
B
C
D
% Relative Abundance
m/z
DPA 170
NnDPA 199
DBP 279
EC 269
'DBP 448
trace amounts of EC present
2EC + Na 559
2EC 537
'DBP 569, 575, 579, 585
NnDPA 199, 4-NDPA 215
296, 317
244, 265
470, 475
564, 579
339, 356
616, 638, 654
669
676
713

Figure 5.3 (continued)

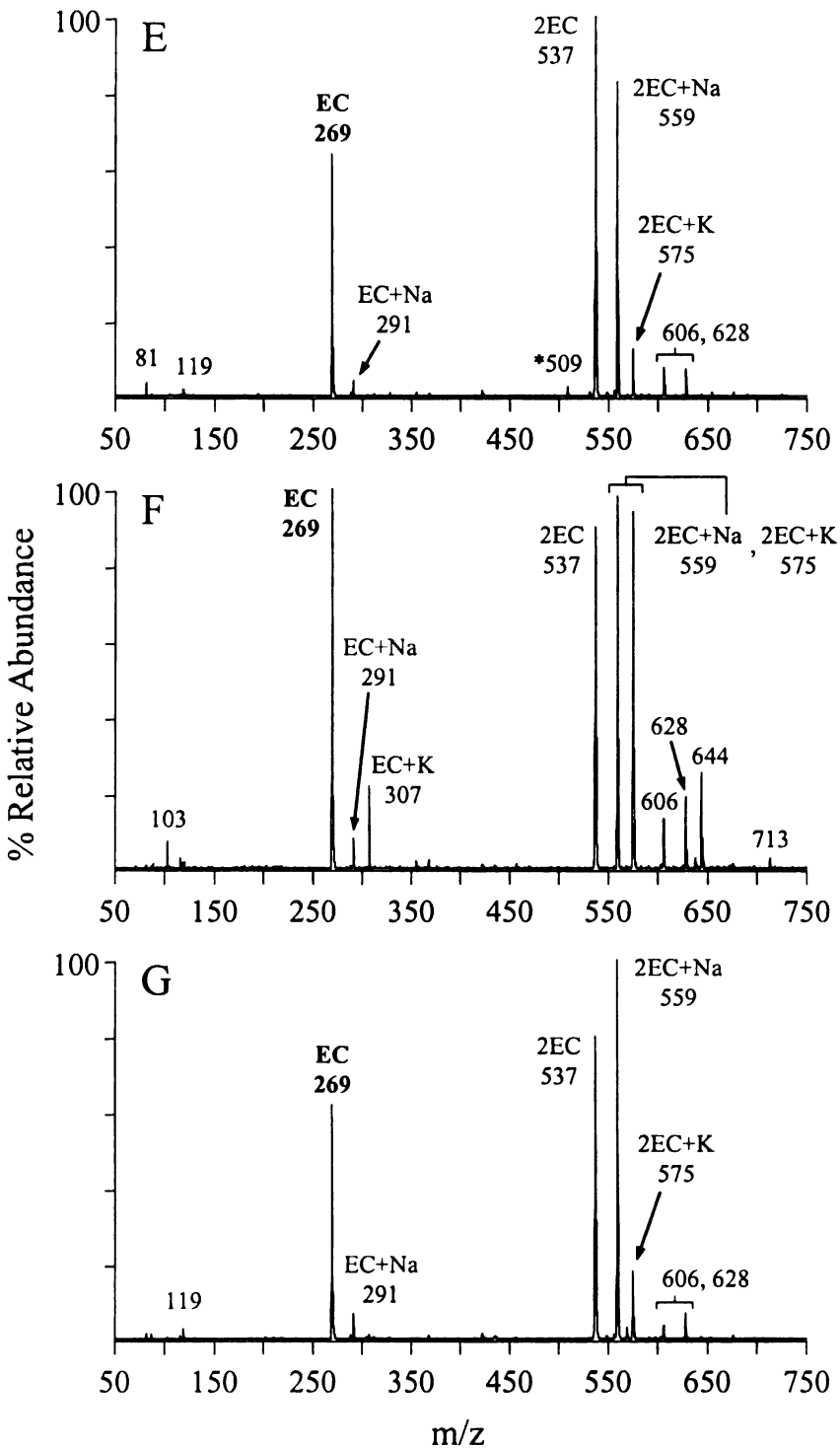

Figure 5.3 Mass spectra for gunpowders (A) #1, (B) # 6, (C) # 3, (D) #5, (E) #2, (F) #4, and (G) #7 at concentrations of 0.1 mg/mL extracted material in methanol.

At first glance, it is apparent that powders 2, 4, and 7 (Figures 5.3E, 5.3F, and 5.3G, respectively) yield mass spectra that are very similar to each other, primarily differing only in the abundance of EC adduct ions. These spectra are very different than those seen for powders 1, 3, 5, and 6, which contain EC and DPA as well as many other peaks not seen for powders 2, 4, and 7. This is consistent with the similarities seen before with morphology and extractability. By examining the composition of each of the powders more closely, further distinction can be made between them, as discussed in the following section. Table 5.2 gives a condensed list of the MS and MS^n data for the powders, as it lists only those peaks that could be identified in some manner. A complete list of the mass spectrometry data for powders 1-7 can be found in Tables A.1 – A.7, respectively, in the Appendix.

Table 5.2 MS and MS^n data for identified peaks in the smokeless powder samples.

Component	Powder component present in	Precursor ions (m/z)	MS/MS product ions (m/z) (% relative abundance)	MS^3 product ions (m/z) (% relative abundance)	MS^4 product ions (m/z) (% relative abundance)
EC	1, 2, 3, 4, 5, 6, 7	269	120 (14%) 148 (100%)	120 (100%)	92 (100%)
EC+Na	2, 4, 7	291			
EC+K	4	307			
*EC	2	509	269 (100%)	120 (5%) 148 (100%)	
*EC	3	602	269 (100%)	120 (10%) 148 (100%)	
*EC	1	606	269 (100%)	120 (8%) 148 (100%)	
*EC	1, 2, 4, 7	628	291 (100%) 360 (82%) 457 (32%)		
2EC	1, 2, 4, 7	537	269 (100%)	120 (9%) 148 (100%)	
2EC+Na	1, 2, 4, 7	559	291 (100%)		
2EC+K	4	575	307 (100%)		
DPA	1, 3, 5, 6	170	92 (100%)		
N-NO-DPA	1, 5, 6	199	169 (100%)	65 (45%) 104 (100%)	
4-NDPA	6	215	198 (100%)	168 (100%)	
DPA-like component	3	227	170 (75%) 196 (100%)	92 (100%) 168 (100%)	
2DPA-like component	3	453	227 (100%)	170 (70%) 196 (100%)	

Table 5.2 (continued)

°DPA-like component	3, 5	317	149 (28%) 227 (10%) 271 (100%) 299 (46%)	 170 (68%) 196 (100%) 253 (40%) 271 (100%)	
DBP	1, 3, 5, 6	279	149 (20%) 204 (100%)	 149 (100%)	
'DBP	1	575	279 (100%)	149 (10%) 204 (100%)	
'DBP	1	585	279 (100%)	149 (14%) 204 (100%)	
'DBP	5, 6	448	279 (100%)	149 (8%) 204 (100%)	

*Unidentified EC adduct/complex, ° Unidentified DPA-like component adduct/complex, ' Unidentified DBP adduct/complex

None of the powders contained MC, which is most likely due to where the powders used in this study were manufactured, as MC is more commonly used than EC as a stabilizer in Chinese gunpowder [31]. With the increase of terrorism [10], however, it would not be unlikely for a forensic analyst to encounter smokeless powder containing MC. Since the MC and EC standards behaved almost identically due to their similar structures (Chapter 4), though, it is likely that MC in smokeless powder would be detectable by this nESI-MS technique. Since none of the powders contained MC, they all did, as might be expected, contain EC to some extent. The amount of EC in powder 3, however, was so minute that it was only detectable using SRM, illustrating the power of that scan type. For some of the powders there were EC containing complexes that could not be specifically identified, but whose fragmentation behavior suggested the presence

of EC; these compounds are marked with a " * " in Tables 5.2 and A.1-A.7. Powders 2, 4, and 7 contained only EC, but powders 1, 3, 5, and 6 contained the stabilizer DPA in addition to EC. By seeing both EC and DPA in powders 1, 3, 5 and 6, the probability that the powders are smokeless powder increases significantly.

Powders 1, 5, and 6 contained N-nitrosodiphenylamine (N-NO-DPA, protonated in Structure 4 of Scheme 5.1), while powder 6 also contained 4-nitrodiphenylamine (4-NDPA, Structure 5). The presence of these compounds was confirmed by performing MS/MS and MS^3 and through comparison with known fragmentation behavior given in literature [29]. As an example, the possible mechanism for protonated N-NO-DPA fragmentation is given in Scheme 5.1. Both N-NO-DPA and 4-NDPA are nitrated derivates of DPA [11, 14, 29], which provide strong evidence that the powder being analyzed is the explosive smokeless powder.

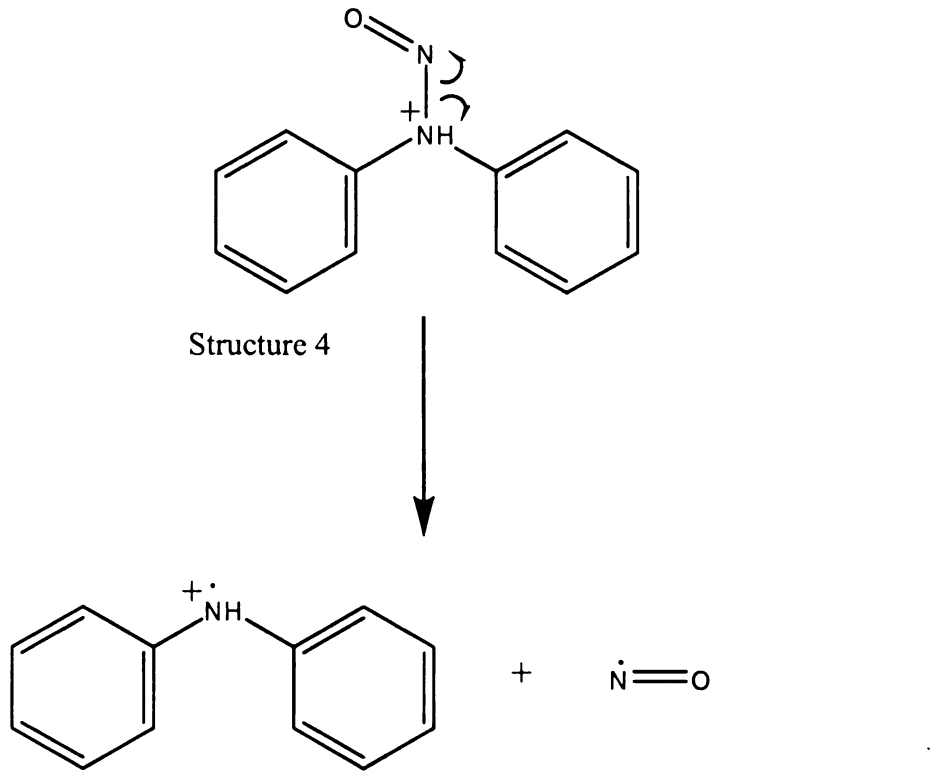

Structure 4

Scheme 5.1 Possible mechanism for the fragmentation of protonated N-nitrosodiphenylamine (N-NO-DPA, Structure 4) to form a product ion at m/z 169.

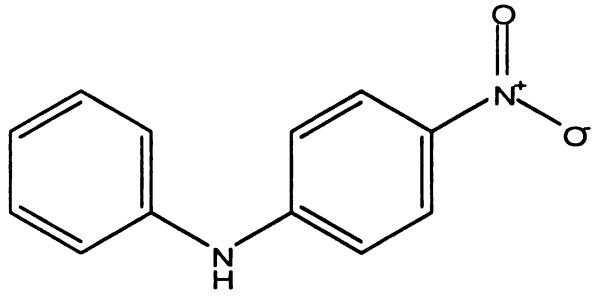

Structure 5: 4-nitrodiphenylamine (4-NDPA)

Powders 1, 3, 5 and 6 also contained the plasticizer dibutyl phthalate (DBP, Structure 6). DBP has very little forensic value alone as it is used widely in a variety of products other than smokeless powder. However, seeing DBP in conjunction with EC

and DPA, adds further certainty that the unknown substance being analyzed is smokeless powder. As was the case for EC, there were some peaks that are most likely DBP adducts or complexes based on their fragmentation behavior, but these peaks were not specifically identified; these peaks are marked with a " ′ "in Tables 5.2 and A.1-A.7.

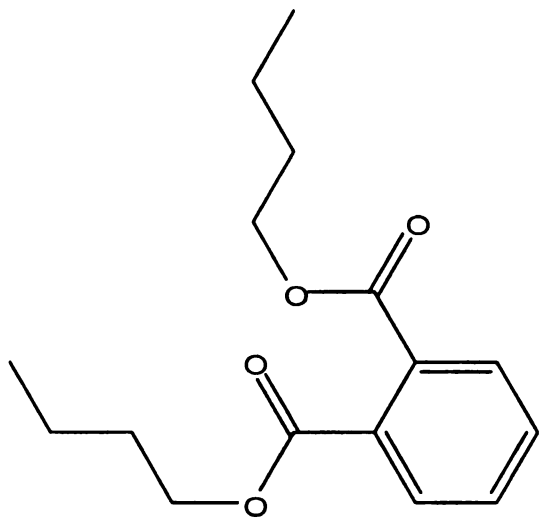

Structure 6: Dibutyl phthalate (DBP)

Powder 3 contains an ion at m/z 227, which is not seen for any of the other powders. This ion fragments to yield product ions at m/z 170 and m/z 196. The product ion at m/z 170 fragments to yield an ion at m/z 92, the fragmentation pathway seen for DPA, while the product ion at m/z 196 fragments to yield m/z 168. This would suggest that the ion at m/z 227 could be a DPA-like ion in structure. One possibility is a DPA-glycine derivative compound that has protonation at two different sites (Structure 7).

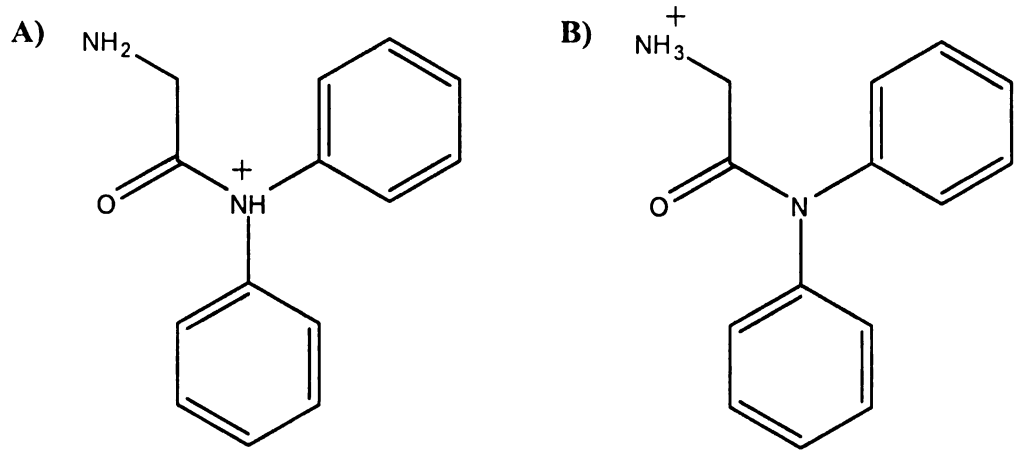

Structure 7: Possible protonated isomers of the DPA-like species at m/z 227.

The loss of NH_2CH_2CO plus a H^+ transfer from isomer (A) in Structure 7 could lead to the protonated DPA structure, $[NHC_{12}H_{10} + H]^+$, at m/z 170, which would fragment accordingly (Scheme 4.3). A proton transfer would result in isomer (B) in Structure 7, which could lose NH_2CH_2 to form the product ion at m/z 196, $[NC_{12}H_{10}CO]^+$, while the further loss of CO would yield the ion at m/z 168, $[NC_{12}H_{10}]^+$. Confirmation of the exact structure of the ion at m/z 227 is beyond the scope of this project, but forensically, even without knowing the exact composition, the ion at m/z 227 can help to distinguish between powders. Powder 5 does not contain the ion at m/z 227, but it does have an ion at m/z 317 (also seen for powder 3) that fragments to yield 227, which in turn dissociates to give ions at m/z 170 and 196. This would suggest that the ion at m/z 317 is a complex consisting partly of the ion at m/z 227 or that the ion at m/z 227 is a product ion of the ion at m/z 317 inadvertently formed by in-source fragmentation.

A summary of the main components present in the powders is given in Table 5.3. It is easy to see that all seven powders would be able to be identified as being smokeless powders based on the components detected by this method. Comparisons can also be

made based on composition as powders 2, 4, and 7 do not contain DPA or DBP, while powders 1, 3, 5, and 6 do. Also, powders 3 and 5 contain the DPA-like component, which can be used to separate them from other powders.

Table 5.3 Stabilizers and other components detected in smokeless powder samples by nESI quadrupole ion trap mass spectrometry.

Powder	EC	DPA	DBP	DPA-like component (m/z 227)
1 (9 mm)	x	x	x	
2 (9 mm +P)	x			
3 (0.45 ACP, JHP)	x	x	x	x
4 (0.45 ACP, FMJ)	x			
5 (0.40 S&W, Fed.)	x	x	x	x (only seen in complex)
6 (0.40 S&W, Win.)	x	x	x	
7 (.357 Magnum)	x			

Spectra were also acquired for all seven powders extracted in deionized water. This was done because water is the most likely solvent a powder or residue will come in contact with in the real world. Since the extraction efficiency was much less than it was for the methanol extracted solutions (Table 5.1), no dilutions were performed. EC was detected for powders 1, 2, 4, and 7, while DPA was detected in powder 5. Neither component was identified for powders 3 or 6. This is likely do to the low extraction yield in water and that different powders will have different concentrations of components, *i.e.*, powders 1, 2, 4, and 7 possibly contain more EC than the other powders. Where EC and

DPA were detected, the relative abundance of their peaks was low. This combined with the fact that these solutions were not diluted, indicates that neither compound is very soluble in water. This is forensically significant because it reduces the chances of these components being washed off a piece of evidence by water, such as rain. The mass spectra for powders 1, 3, 5, and 6 in water also showed a series of peaks differing by a mass of 100. Tandem mass spectrometry experiments showed that these peaks were fragment peaks, such that some compound was consistently losing a mass of 100. This compound is therefore most likely a polymeric plasticizer and when seen alone is of little forensic value. Since water did not have a high extraction efficiency and it yielded no new significant peaks, methanol is the best solvent to use for the extraction of organic components from debris or submitted samples.

5.5 Analysis of Gunshot Residue by nESI-MS

The smokeless powders previously analyzed by nESI-MS were fired into cloth squares at distances of 3″ and 12″. Unwashed ('as is' from the package), washed with deionized water and air dried, and machine washed and dried cloth were used. Unwashed and machine washed samples were used to represent 'real world' conditions. Cloth extensively washed with deionized water was used to remove any contaminants and thus minimize the background, so that if any new peaks were seen compared to the unburned powder the new peaks would be clearly visible above the noise. As an example, Figure 5.4 shows the spectra for gunshot residue obtained from powder 2 (9 mm +P) on these various cloths. Powder 2 contains EC, but not DPA.

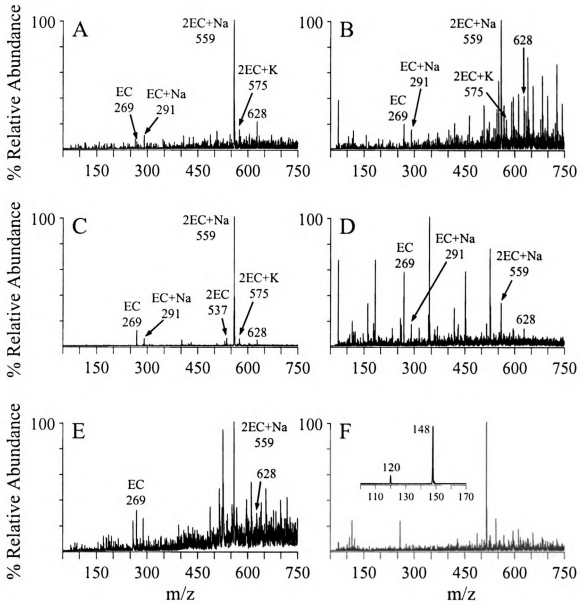

Figure 5.4 Mass spectra for gunshot residue from smokeless powder 2 (9 mm+P): (A) firing distance of 3″ on unwashed cloth, (B) firing distance of 12″ on a unwashed cloth, (C) firing distance of 3″ on cloth washed with deionized water, (D) firing distance of 12″ on cloth washed with deionized water, (E) firing distance of 3″ on machine washed cloth, and (F) firing distance of 12″ on machine washed cloth. The inset to Figure 5.4F shows the region of m/z from 100 to 170 acquired by performing MS/MS on the m/z 269 protonated precursor ion.

On unwashed cloth (Figure 5.4A and 5.4B) peaks can be seen at the higher m/z values. These peaks could be from a detergent used in the manufacturing process as the substance was removed by washing the cloth in water upon which the water became slightly sudsy. For both spectra, the most abundant peak in the spectrum was $[2EC+Na]^+$at m/z 559. At the 3″ firing distance (Figure 5.4A), however, the abundance of the peaks from the cloth (*i.e.*, the possible detergent peaks) appears to be less than it is for the cloth fired upon at a 12″ firing distance (Figure 5.4B). Less gunshot residue will be deposited the longer the firing distance is. Therefore, the detergent peaks are the same abundance in both spectra, only the abundance of the EC peaks is changing, *i.e.*, less abundant at the farther firing distance of 12″.

Figures 5.4C and 5.4D show the spectra for gunshot residue obtained at firing distances of 3″ and 12″, respectively, on cloth cleaned with deionized water. With the detergent peaks eliminated, the most abundant peaks in the spectrum at 3″ are from EC. No additional peaks are seen when compared to the spectra for the unburned powder 2 (Figure 5.3E). At 12″, peaks for EC can easily be seen, but their abundance is, as expected, significantly lower than it was at 3″ such that background ions are seen at high abundances.

Cloth was also machined washed and dried as the most realistic example of cloth that would be encountered in a forensic setting. Both the spectrum at 3″ (Figure 5.4E) and the spectrum at 12″ (Figure 5.4F) show some background ions probably attributable to detergent, but not as much as was present for the unwashed fabric (Figures 5.4A and B). At 3″ (Figure 5.4E), EC peaks are distinguishable among the other background and detergent peaks, but at 12″ (Figure 5.4F), any EC peaks that may be present were in the

noise and thus not detectable. When MS/MS, however, was performed on the low abundant ion at m/z 269 that was present, the characteristic product ions of EC at m/z 120 and 148 formed (inset to Figure 5.4F), proving that EC was present, but at low concentration. This shows the utility of tandem mass spectrometry for the identification of trace amounts of material in a complex matrix.

The advantages of using SRM are also exemplified with the gunshot residue spectra. Figure 5.5 shows the spectra for unwashed cloth without gunshot residue (a blank) (Figure 5.5A) and unwashed cloth with gunshot residue from powder 1 (9 mm) at a firing distance of 12″ (Figure 5.5C). Both spectra show large detergent peaks, the most abundant of which range from m/z 463 to m/z 777, but neither spectra show a peak at m/z 269 above the S/N ratio. MS/MS on the protonated precursor ion at m/z 269 from the blank yielded product ions at m/z 187 and 239 (Figure 5.5B). This indicates that the blank does not contain EC, but has a contaminant at that same m/z as protonated EC (m/z 269). MS/MS on the protonated precursor ion at m/z 269 from the cloth with gunshot residue gives the product ions at m/z 120, 148, 187 and 239. The product ions at m/z 120 and 148 are consistent with EC (confirmed by MS^3), while the ions at m/z 187 and 239 are from the contaminant in the cloth (compare Figures 5.5B and 5.5D). This exemplifies the value of SRM, where the fragmentation pathway 269 → 148 could be monitored and any peaks from the contaminant ion at m/z 269 not be shown. As the concentration of EC decreases on the cloth, as would happen at longer firing distances, the product ions at m/z 120 and 148 would decrease to the point that eventually the product ions from the contaminant at m/z 187 and 239 would overshadow the product ions of interest. SRM

would then be crucial for confirming the presence of EC in a powder because it improves selectivity by eliminating interferences.

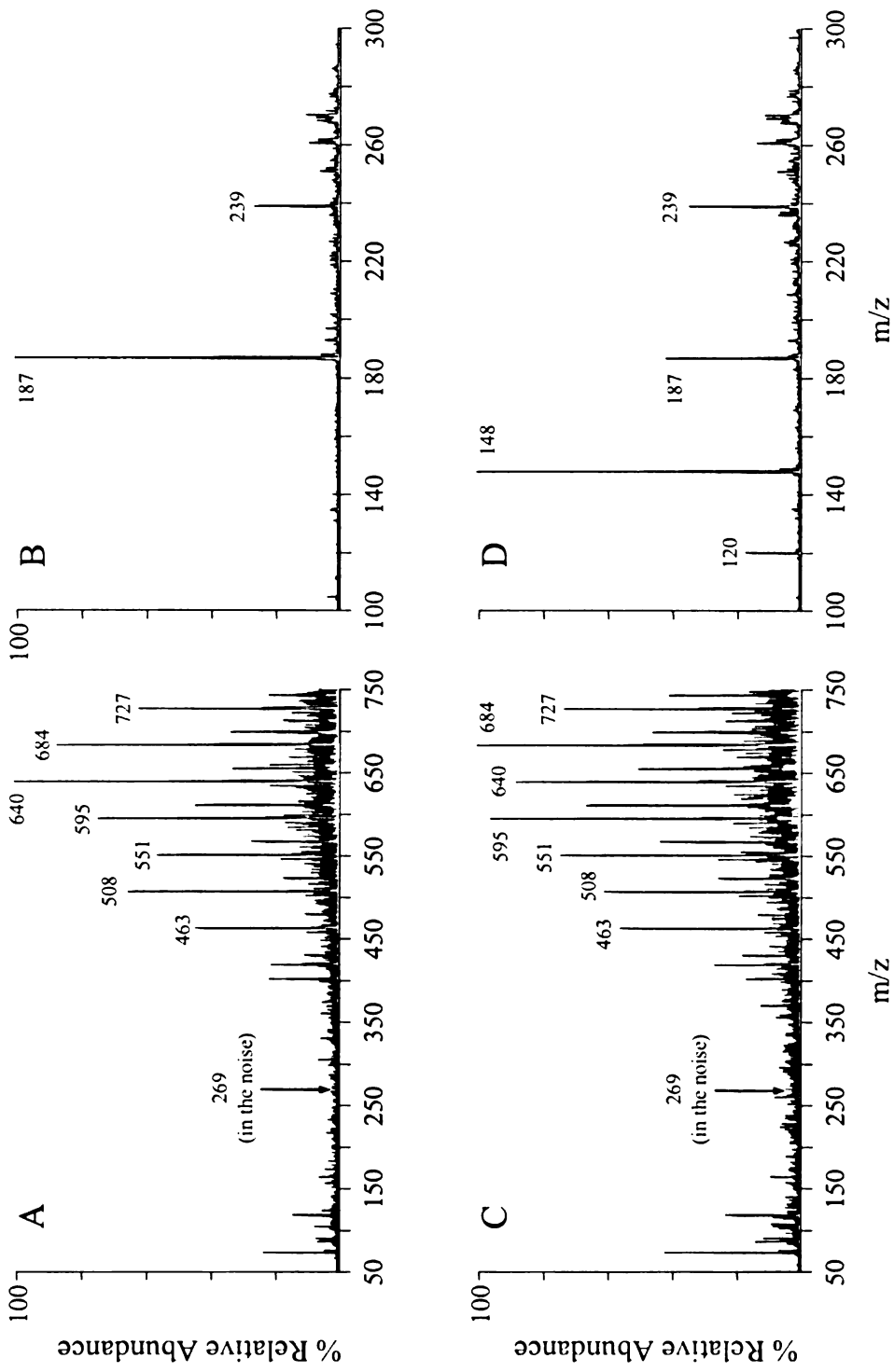

Figure 5.5 Comparison of mass spectra for unwashed cloth with and without gunshot residue. (A) Mass spectra of unwashed cloth (blank). (B) MS/MS product ion spectrum of the ion at m/z 269 in Figure 5.5A. (C) Mass spectra of gunshot residue from smokeless powder 1 (9 mm) on unwashed cloth (firing distance of 12"). (D) MS/MS product ion spectrum of the ion at m/z 269 in Figure 5.5C.

Results similar to those discussed above for the residues from powders 1 and 2 were seen for all the other powders' residues. The main compounds seen for each powder's residue are summarized in Table 5.4. By comparing this table to Table 5.3, it is apparent that every component seen in the unburned powder is also seen in the residue, except for the DPA-like component (powder 5) and nitrated derivatives of DPA (powders 1, 5, and 6). This is most likely because in unburned powder these components were only present at trace levels, so when in residue form, the concentration of these components fell below the LODs. Thus, this technique can be used not only for the identification of a powder or residue as smokeless, but it can also be used to compare unburned powder with burned powder based on compositional differences.

Table 5.4 Stabilizers and other components detected in smokeless powder gunshot residue (firing distances: 3″ and 12″) by nESI quadrupole ion trap mass spectrometry.

Residue	EC	DPA	DBP	m/z 227
1 (9 mm)	x	x	x	
2 (9 mm +P)	x			
3 (0.45 ACP, JHP)	x	x	x	x
4 (0.45 ACP, FMJ)	x			
5 (0.40 S&W, Federal)	x	x	x	
6 (0.40 S&W, Winchester)	x	x	x	
7 (.357 Magnum)	x			

5.6 Summary

Seven smokeless powder samples were analyzed by stereomicroscopy, extraction properties, and nESI-MS. For all powders, nESI-MS was able to identify them as being smokeless powder. By combining the data for all analyses, it is possible to differentiate many of the powders from one another. This would be forensically useful when comparing unburned powder from a crime, be it an unexploded IED or an unfired cartridge, to powder found with a suspect.

Based on physical attributes powders 1, 3, 5, and 6 can be separated from powders 2, 4, and 7. It is interesting to note that the two 9 mm cartridges fall into separate groupings, as do the two 0.40 cartridges. Powders 1 and 6 and powders 3 and 5 show subtle similarities. Powder 3 has a distinct rough texture but not different enough for a conclusive inclusion or exclusion when compared to powders 1, 5, and 6. Powder 7 can definitively be differentiated from powders 2 and 4. From the extraction data, powders 1 and 6 are similar, powders 3 and 5 are similar, and powders 2, 4, and 7 are similar. This allows another level of differentiation between powders 1, 3, 5, 6 and powders 2, 4, 7, and also helps to distinguish powders 1 and 6 from powders 3 and 5 by combining this data with the physical characteristic differences.

The mass spectrometry data further differentiated among powders 1, 3, 5, and 6, which contained EC, DPA, and DBP, and powders 2, 4, and 7, which contained only EC. Powder 3 also contained a unique ion at m/z 227, which was seen in a possible adduct form for powder 5. Powder 6 also contained two nitrated DPA (N-NO-DPA and 4-NDPA) compounds allowing it to be differentiated from the other powders. Powders 1 and 5 contained one nitrated DPA product (4-NDPA). Overall, by combining all of the

data every powder could be distinguished from the others with the exception of powders 2 and 4, which could be evidence that these two powders are actually the same powder that is packaged differently – in a 9 mm +P by Federal and in a 0.45 ACP by Federal.

The organic stabilizers MC, EC, and DPA in gunshot residue obtained from the seven smokeless powders was examined by tandem mass spectrometry (MS/MS and MS^3) in a quadrupole ion trap using nESI in order to explore the utility of this method for the routine and rapid identification of gunshot residue. This technique was able to identify GSR at both firing distances (3″ and 12″) on all types of cloth – unwashed, washed in deioinzed water, and machine washed. The use of tandem mass spectrometry and SRM scan type increased the selectivity of this technique and allowed for the identification of components that would otherwise not be seen. This method should also work for the identification of smokeless powder in post-blast residue.

CHAPTER SIX

Conclusions and Future Directions

6.1 Conclusions

The detection of explosives and their residues is a crucial aspect of forensic science. Smokeless powder is the most common explosive used in firearm cartridges today. It is also widely used in improvised explosive devices (IEDs), such as pipe bombs, because of its wide commercial availability as gunpowder. The determination of the presence of any gunshot residue (GSR) at firearm incidents is forensically important, as this can help aid in the identification of suspects, the determination of cause/manner of death, in establishing a scenario of events and so forth. Similarly, the analysis of post-blast residue from an IED can help determine the type of explosive used, which in turn can greatly aid in the generation of a list of suspects. Unburned powder can also have forensic significance, as powder found at the scene of a crime (be it a firearm related incident or an unexploded IED) can be directly compared to powder found with a suspect. Comparisons can also be made between residues at a crime scene and any unburned powder from a suspect.

The stabilizers commonly found in smokeless powder, methyl centralite (MC), ethyl centralite (EC), and diphenylamine (DPA), are considered to be the most unique organic components of smokeless powder. Analysis of these components not only allows one to identify GSR, but it can also be used to help identify the explosive used in an IED and, if a suspect powder is available, comparisons can be made. The ability to yield different information from a single forensic analysis is an advantage for forensic

laboratories. The work presented here was designed to be a preliminary examination of the feasibility of electrospray ionization mass spectrometry (ESI-MS) for the detection of smokeless powder and its residue by specifically targeting the compounds MC, EC, and DPA.

Initially, standard solutions of MC, EC, and DPA were used to successfully optimize the nESI-MS conditions for the simultaneous detection of all three stabilizers, as in a 'real world' case it would not initially be known which, if any, of these compounds were present. Upon analysis of the mass spectra for the standard solutions, it could be seen that the key fragmentation pathway for MC was m/z 241 to m/z 134, while the protonated precursor ion for EC at m/z 269 dissociated to give m/z 148, and likewise DPA fragmentated from m/z 170 to m/z 92. These known fragmentation pathways could then be used with selected reaction monitoring (SRM) to increase the selectivity of this technique and thus the ability to detect trace components. Limits of detection (1 fmol/μL for MC and EC, 10 fmol/μL for DPA) were obtained for all three components by utilizing the tandem capabilities of the ion trap mass spectrometer and the selected reaction monitoring scan type.

Samples of smokeless powder were obtained from seven different firearm cartridge types. An initial physical comparison of the powders showed that powders 1, 3, 5, and 6 had similar traits, as did powders 2, 4, and 7. Powder 7, however, was the only powder that could be distinguished from the others based solely on physical characteristics, highlighting the need for compositional analysis by mass spectrometry. An efficient, yet rapid, extraction method for small amounts of smokeless powder in methanol was developed. In doing this, however, another set of data was obtained that

could further differentiate the powders. It could be seen that powders 1 and 6, powders 3 and 5, and powders 2, 4 and 7 had comparable extraction tendencies, indicating that they had similar methanol soluble components.

The nESI-MS spectra obtained for the seven smokeless powders under optimized conditions further distinguished powders 2, 4 and 7 from the other powders, as powders 2, 4, and 7 contained only EC, while powders 1, 3, 5, and 6 contained EC, DPA, and the plasticizer dibutyl phthalate (DBP). MC was not detected in any of the powders. Further differentiation could be obtained as powders 3 and 5 contained an unidentified compound that is DPA-like in structure. Powders 1 and 5 contain one nitrated DPA derivative (4-NDPA), while powder 6 contained this derivate and the nitrated DPA derivative N-NO-DPA. By combining all of the data (physical characteristics, extraction efficiency, and mass spectra), it was possible to differentiate all the powders, except powders 2 and 4, indicting that powders 2 and 4 could be from the same manufacturer. It was also possible to confirm each powder as being smokeless powder. The presence of multiple components in powders 1, 3, 5, and 6 increased the certainty of the identification of these powders as being smokeless powder. Nitrated derivatives of DPA, seen for powders 1, 5, and 6, are thought to be especially unique to smokeless power.

Gunshot residue was obtained for the seven powders at firing distances of 3″ and 12″. The powders were fired into unwashed, washed with deionized water and air dried, and machine washed and dried cloth. EC was detected for all powders at both firing distances and on all cloth types, while EC, DPA, and DBP were detected for powders 1, 3, 5, and 6 at both distances and on all cloth types. None of the nitrated derivatives of DPA were detected. This is most likely because these derivatives were present only at

trace levels in the powder form and would therefore be at even smaller concentrations in the residue form. The utility of tandem mass spectrometry and SRM was illustrated by the presence of a contaminate ion at m/z 269 (the m/z for protonated EC) on unwashed cloth. In all cases, the residue could be identified as being GSR produced by smokeless powder, demonstrating that the LODs for this technique are good. Additionally, some compositional comparisons can be made between the residue and the previously analyzed unburned powder, as, for example, powder 1 could be eliminated as the source for the GSR produced by powder 2 as powder 1 contains DPA and DBP, but powder 2's GSR did not contain either of these compounds. This technique could also be applied to post-blast residue from an IED or similar explosive device.

6.2 Future Directions

As this work successfully developed a method of the analysis of smokeless powder by nESI-MS and demonstrated its utility with 'real world' samples, there are now many other aspects that could be examined. More smokeless powder samples could be obtained from different cartridges in order to start developing statistical data on the frequency certain components are present and to determine what powders contain the stabilizer MC, as it was not detected for any of the powders used in this study. Powder packaged for reloading purposes could also be examined in order to determine differences between this powder and powders obtained from cartridges. Different batches of powder could be examined to assess the effect of 'rework' on compositional analysis.

Since GSR was detected on all three cloth types and at both firing distances used in this study, it would be worthwhile continuing this aspect of the project. Different firing distances could be used to determine the maximum distance detectable with this method. GSR on different mediums, such as colored fabric, different types of fabric, plastic, and skin, could also be studied. There is also the issue of the persistence of GSR on cloth. Cloth stored in different conditions, over different amounts of time could be examined. Also, different handling of the GSR containing cloth could be examined, such as brushing the cloth or even washing it [13]. The effect of different contaminants, such as blood and dirt, could be studied. IEDs could be built with smokeless powder in order to analyze this residue and see if it differs from that obtained for GSR. Overall, this project has laid the foundation for many avenues of future forensic work in the detection of smokeless powder.

APPENDIX

Table A.1 Complete MS and MS^n data for smokeless powder sample 1.

Component	Precursor ions (m/z)	MS/MS product ions (m/z)	MS^3 product ions (m/z)
Unidentified	103		
DPA	170	92	
N-NO-DPA	199	169	66 104
EC	269	120 148	 120
DBP	279	149 205	 149
Unidentified	296	250 257 277 279 295 307 314	
° DPA-like component	317	149 227 271 299	 170 197 253 271
Unidentified	355	338	303 321
Unidentified	425	181 288 321 348	
2EC	537	269	120 148
Unidentified	548	515	

Table A.1 (continued)

2EC+Na	559	291	
Unidentified	569	301	
′DBP	575	279	149 204
Unidentified	579	301	
′DBP	585	279	149 204
Unidentified	595	301	
*EC	606	269	120 148
Unidentified	616		
*EC	628	291 360	
Unidentified	638	301	
Unidentified	644	301	
Unidentified	654	315	

* Unidentified EC adduct/complex
° Unidentified DPA-like component adduct/complex
′ Unidentified DBP adduct/complex

Table A.2 Complete MS and MS^n data for smokeless powder sample 2.

Component	Precursor ions (m/z)	MS/MS product ions (m/z)	MS^3 product ions (m/z)
Unidentified	82		
Unidentified	119		
EC	269	120 148	 120
EC+Na	291		
Unidentified	355	269 288 322 338 353	
Unidentified	422	288	
*EC	509	269	120 148
Unidentified	531		
2EC	537	269	120 148
Unidentified	548	515	
Unidentified	557		
2EC+Na	559	291	
Unidentified	575	305	
Unidentified	606	436	
*EC	628	291 360 457	 288
Unidentified	654	315	
Unidentified	676	338	303 321

* Unidentified EC adduct/complex

Table A.3 Complete MS and MS^n data for smokeless powder sample 3.

Component	Precursor ions (m/z)	MS/MS product ions (m/z)	MS^3 product ions (m/z)
Unidentified	88		
Unidentified	103	39	
DPA	170	92	
DPA-like component	227	170 196	92 168
Unidentified	244	227	
Unidentified	265		
EC	269	120 148	 120
DBP	279	149 205	 149
° DPA-like component	317	149 227 271 299	 170 197 253 271
Unidentified	355	338	303 321
Unidentified	425	237 265	
2DPA-like component	453	227	170 196
Unidentified	470	170 354	
Unidentified	475	249	
Unidentified	491	265	
Unidentified	527	249	301
Unidentified	543	264	
Unidentified	564	227	
Unidentified	579	301	

Table A.3 (continued)

Unidentified	595	301	
*EC	602	269	120 148
Unidentified	638	301	
Unidentified	654	315	
Unidentified	713	591 636 667	423 468 590

* Unidentified EC adduct/complex

° Unidentified DPA-like component adduct/complex

Table A.4 Complete MS and MS^n data for smokeless powder sample 4.

Component	Precursor ions (m/z)	MS/MS product ions (m/z)	MS^3 product ions (m/z)
Unidentified	102		
EC	269	120 148	 120
EC+Na	291		
EC+K	307		
Unidentified	355	269 288 322 338 353	 303 320
Unidentified	368		
Unidentified	422	288	181 223 274
Unidentified	457	288	
2EC	537	269	120 148
2EC+Na	559	291	
2EC+K	574	307	
Unidentified	606	436	
*EC	628	291 360 457	
Unidentified	644	306	
Unidentified	713	591 636 667	423 468 590

* Unidentified EC adduct/complex

Table A.5 Complete MS and MS^n data for smokeless powder sample 5.

Component	Precursor ions (m/z)	MS/MS product ions (m/z)	MS^3 product ions (m/z)
Unidentified	103		
Unidentified	116	100	
DPA	170	92	
N-NO-DPA	199	169	66 104
Unidentified	237	207	
EC	269	120 148	 120
DBP	279	149 205	 149
° DPA-like component	317	149 227 271 299	 170 197 253 271
Unidentified	339		
Unidentified	355	338	
Unidentified	376	206	
Unidentified	425	181 237 265 364	
'DBP	448	279	149 204
Unidentified	517	254 332 347 424 438	
Unidentified	574	305	

Table A.5 (continued)

Unidentified	579	301	
Unidentified	595	315	
Unidentified	616		
Unidentified	638	301	
Unidentified	654	317	
Unidentified	664	607	
Unidentified	669	591	346 423
Unidentified	676		
Unidentified	686	408	
Unidentified	697	619	
Unidentified	702		
Unidentified	713	591 636 667	423 468 590

° Unidentified DPA-like component adduct/complex
′ Unidentified DBP adduct/complex

Table A.6 Complete MS and MS^n data for smokeless powder sample 6.

Component	Precursor ions (m/z)	MS/MS product ions (m/z)	MS^3 product ions (m/z)
Unidentified	103		
DPA	170	92	
N-NO-DPA	199	169	
4-NDPA	215	198	168
EC	269	120	
		148	120
DBP	279	149	
		205	149
Unidentified	296	250	
		257	
		277	
		279	
		295	
		307	
		314	
Unidentified	317	275	
Unidentified	355	338	303
			321
Unidentified	418	401	201
			255
Unidentified	425	181	
		321	
		347	
		369	
'DBP	448	279	149
			204

Table A.6 (continued)

Unidentified	517	254 332 347 423 438 488	 255 332 346 361 410
Unidentified	574	456 556	
Unidentified	579	301	
Unidentified	595	315 515	
Unidentified	616		
Unidentified	638	301	
Unidentified	654	317	
Unidentified	690		

' Unidentified DBP adduct/complex

Table A.7 Complete MS and MS^n data for smokeless powder sample 7.

Component	**Precursor ions (m/z)**	**MS/MS product ions (m/z)**	**MS^3 product ions (m/z)**
Unidentified	82		
Unidentified	119		
EC	269	120 148	 120
EC+Na	291		
Unidentified	422	288	
2EC	537	269	120 148
2EC+Na	559	291	
Unidentified	575	305	
Unidentified	606	436	
*EC	628	291 360	
Unidentified	676	338	303 321

* Unidentified EC adduct/complex

REFERENCES

1. Yinon, J.; Zitrin, S. Modern methods and applications in analysis of explosives, John Wiley and Sons, Chinchester, 1993.

2. Yinon, J. Forensic and Environmental Detection of Explosives, John Wiley and Sons, Chinchester, 1999.

3. National Research Council, Committee on smokeless and black powder. Black and smokeless powders: technologies for finding bombs and the bomb makers, National Academy Press, Washington, D.C., 1998.

4. Saferstein, R. Criminalistics: An introduction to forensic science, 6th edition, Prentice Hall, New Jersey, 1998.

5. Mathis, J. A.; McCord, B. R. Mobile phase influence on electrospray ionization for the analysis of smokeless powders by gradient reversed phase high-performance liquid chromatography-ESIMS. *Forensic Sci. Int.* **2005**, *154*, 159-166.

6. Wallace, C. L.; Midkiff, C. R. Jr. Smokeless powder characterization an investigative tool in pipe bombings. In: Yinon, J., editor. Advances in the analysis and detection of explosives, Kluwer Academic Publishers, Boston, 1993, 29-39.

7. U.S. Department of Justice, Bureau of Justice, Homicide trends in the U.S., http://www.ojp.usdoj.gov/bjs/homicide/weapons.htm, accessed July 2, 2007.

8. Schwoeble, A. J.; Exline, D. L. Current methods in forensic gunshot residue analysis, CRC Press, Boca Raton, 2000.

9. Ammunition Basics Booklet, Federal Cartridge Company, U.S.A., 2006.

10. National Counterterrorism Center, U.S.A., NCTC Report on Terrorist Incidents, 2006.

11. Andrasko, J. Characterization of smokeless powder flakes from fired cartridge cases and from discharge patterns on clothing. *J. Forensic Sci.* **1992**, *37*, 1030-1047.

12. Meng, H.; Caddy, B. Gunshot residue analysis – a review. *J. Forensic Sci.* **1997**, *42*, 553-570.

13. Zeichner, A. Recent developments in methods of chemical analysis in investigations of firearm-related events. *Anal. Bioanal. Chem.* **2003**, 376, 1178-1191.

14. Espinoza, E. O'N.; Thornton, J. I. Characterization of smokeless gunpowder by means of diphenylamine stabilizer and its nitrated derivatives. *Anal. Chim. Acta* **1994**, *288*, 57-69.

15. Mach, M. H.; Pallos, A.; Jones, P.F. Feasibility of gunshot residue detection via its organic constituents. Part I: Analysis of smokeless powders by combined gas chromatography-chemical ionization mass spectrometry. *J. Forensic Sci.* **1978**, *23*, 433-445.

16. MacCrehan, W. A.; Reardon, M. R. A qualitative comparison of smokeless powder measurements. *J. Forensic Sci.* **2002**, *47*, 996-1001.

17. MacCrehan, W. A.; Bedner, M. Development of a smokeless powder reference material for propellant and explosives analysis. *Forensic Sci. Int.* **2006**, *163*, 119-124.

18. MacCrehan, W. A.; Reardon, M. R.; Duewer, D. L. Associating gunpowder and residues from commercial ammunition using compositional analysis. *J. Forensic Sci.* **2002**, *47*, 260-266.

19. Reardon, M. R.; MacCrehan, W. A.; Rowe, W. F. Comparing the additive composition of smokeless gunpowder and its handgun-fired residues. *J. Forensic Sci.* **2000**, *45*, 1232-1238.

20. Wissinger, C. E.; McCord, B.R. A gradient reversed phase HPLC procedure for smokeless powder comparison. *J. Forensic. Sci.* **2002**, *47*, 168-174.

21. Mathis, J. A.; McCord, B. R. Gradient reversed-phase liquid chromatographic-electrospray ionization mass spectrometric method for the comparison of smokeless powders. *J. Chromatogr. A* **2003**, *988*, 107-116.

22. MacCrehan, W. M.; Patierno, E. R.; Duewer, D. L.; Reardon, M. R. Investigating the effect of changing ammunition of the composition of organic additives in gunshot residue (OGSR). *J. Forensic Sci.* **2001**, *46*, 57-62.

23. Reardon, M. R.; MacCrehan, W. A. Developing a quantitative extraction technique for determining the organic additives in smokeless handgun powder. *J. Forensic. Sci.* **2001**, *46*, 802-807.

24. Romolo, F. S.; Margot, P. Identification of gunshot residue: a critical review. *Forensic Sci. Int.* **2001**, *119*, 195-211.

25. Zeichner, A.; Eldar, B.; Glattstein, B.; Koffman, A.; Tamiri, T. Muller, D. Vacuum collection of gunpowder residues from clothing worn by shooting suspects, and their analysis by GC/TEA, IMS, and GC/MS. *J. Forensic Sci.* **2003**, *48*, 961-972.

26. Atwater, C. S.; Durina, M. E.; Diroma, J. P.; Blackledge, R. D. Visualization of gunshot residue patterns on dark clothing. *J. Forensic Sci.* **2006**, 51, 1091-1095.

27. King, R. M. The work of the explosives and gunshot residues unit of the forensic science service (UK). In: Yinon, J., editor. Advances in the analysis and detection of explosives, Kluwer Academic Publishers, Boston, 1993, 91-97.

28. Wu, Z.; Tong, Y.; Yu, J.; Zhang, X.; Pan, C.; Deng, X.; Xu, Y.; Wen, Y. Detection of N,N'diphenyl-N,N'-dimethylurea (methyl centralite) in gunshot residues using MS-MS method. *The Analyst* **1999**, *124*, 1563-1567.

29. Tong, Y.; Wu, Z.; Yang, C.; Yu J.; Zhang, X.; Yang, S.; Deng, X.; Xu, Y.; Wen. Y. Determination of diphenylamine stabilizer and its nitrated derivatives in smokeless gunpowder using a tandem MS method. *The Analyst* **2001**, *126*, 480-484.

30. Berberich, D. W.; Yost, R. A.; Fetterolf, D. D. Analysis of explosives by liquid chromatography/thermospray/mass spectrometry. *J. Forensic Sci.* **1988**, *33*, 946-959.

31. Wu, Z.; Tong, Y.; Yu, J.; Zhang, X.; Yang, C.; Pan, C.; Deng, X.; Wen, Y.; Xu, Y. The Utilization of MS-MS method in detection of GSRs. *J. For. Sciences* **2001**, *46*, 495-501.

32. Tamiri, T.; Zitrin, S. Capillary column gas chromatography /mass spectrometry of explosives. *J. Energetic Mater.* **1986**, *4*, 215-237.

33. Druet, L.; Angers, J. LC/MS studies of ethyl centralite stabilized propellants. *Propellants, Explos., Pyrotech.* **1988**, *13*, 87-94.

34. Fenn, J. B.; Mann, M.; Meng, C. K.; Wong, S. F.; Whitehouse, C. M. Electrospray ionization for mass spectrometer of large biomolecules. *Science* **1989**, *246*, 64-71.

35. Gomez, A.; Tang, K. Charge and fission of droplets in electrostatic sprays. *Phys. Fluids* **1994**, *6*, 404-414.

36. Thomson, B. T.; Iribarne, J. V. Field induced ion evaporation from liquid surfaces at atmospheric pressure. *J. Chem. Phys.* **1979**, *71*, 4451-4463.

37. Iribarne, J. V.; Thomson, B. T. On the evaporation of small ions from charged droplets. *J. Chem. Phys.* **1976**, *64*, 2287-2294.

38. Kerbale, P. A brief overview of the present status of the mechanisms involved in electrospray ionization mass spectrometry. *J. Mass Spectrom.* **2000**, *35*, 804-817.

39. Wilm, Matthias; Mann, Matthias. Analytical properties of the nanoelectrospray ion source. *Anal. Chem.* **1996**, *68*, 1-8.

40. Karas, M.; Hillenkamp, F. Laser desorption ionization of proteins with molecular masses exceeding 10 000 Daltons. *Anal. Chem.* **1988**, *60*, 2299-2301.

41. Zenobi, R.; Knochenmuss, R. Ion formation in MALDI mass spectrometry. *Mass Spectrom. Rev.* **1998**, *17*, 337-366.

42. Hoffmann, E. D.; Stroobant, V. Mass spectrometry principles and applications, 2nd edition, John Wiley and Sons, New York, 2002.

43. March, R. E. An introduction to quadrupole ion trap mass spectrometry. *J. Mass Spectrom.* **1997**, *32*, 351-369.

44. McLuckey, S. A.; Goeringer, D. E. Slow heating methods in tandem mass spectrometry. *J. Mass Spectrom.* **1997**, *32*, 461-474.

45. Skoog, D. A.; Holler, F. J.; Nieman, T. A. Principles of instrumental analysis, 5th edition, Thomson Learning, Inc., Australia, 1998.

46. Gilbert-Lopez, B.; Garcia-Reyes, J. F.; Ortega-Barrales, P.; Molina-Diaz, A.; Fernandez-Alba, A. R. Analyses of pesticide residues in fruit-based baby food by liquid chromatography/electrospray ionization time-of-flight mass spectrometry. *Rapid Commun. Mass Spectrom.* **2007**, *21*, 2059-2071.

47. Hager, J. W. A new linear ion trap mass spectrometer. *Rapid Commun. Mass. Spectrom.* **2002**, *16*, 512-526.

48. Schwartz, J. C.; Senko, M. W.; Syka, J. E. A two-dimensional quadrupole ion trap mass spectrometer. *J. Am. Soc. Mass Spectrom.* **2002**, *13*, 659-669.